

Supplementary Information

Radical-Mediated Enzymatic Carbon Chain Fragmentation-Recombination

Qi Zhang¹, Yuxue Li², Dandan Chen¹, Yi Yu¹, Lian Duan¹, Ben Shen³, and Wen Liu^{1*}

¹State Key Laboratory of Bioorganic and Natural Products Chemistry, Shanghai Institute of Organic Chemistry, Chinese Academy of Sciences, 345 Lingling Rd., Shanghai 200032, China

²State Key Laboratory of Organometallic Chemistry, Shanghai Institute of Organic Chemistry, Chinese Academy of Sciences, 345 Lingling Rd., Shanghai 200032, China

³Division of pharmaceutical Sciences, School of Pharmacy, University of Wisconsin-Madison, 777 Highland Ave., Madison, Wisconsin 53705, USA

Corresponding Author: wliu@mail.sioc.ac.cn,

Table of contents

1. Supplementary Methods

1.1 General Materials and Methods.

1.2 Gene Cloning and Expression.

1.3 Protein Purification and Characterization.

1.4 Determination of the Products, Shunt Products, and Intermediate in NosL-Catalyzed Conversion.

1.5 Determination of 5'-fluoro-NOS (**27**).

1.6 Synthesis.

1.7 Theoretical Calculations.

1.8 *In vitro* Susceptibility Testing.

2. Supplementary Results

2.1 Supplementary Figures

Supplementary Figure 1 Time course analysis of MIA production in *nosL*-expressing strain.

Supplementary Figure 2 Multiple sequence alignment of selected radical *S*-AdoMet proteins.

Supplementary Figure 3 HPLC analysis of MIA production in the recombinant *E. coli* strains.

Supplementary Figure 4 Quantitative analysis of NosL-catalyzed *in vitro* conversion.

Supplementary Figure 5 Characterization of the reconstituted NosL.

Supplementary Figure 6 NosL-catalyzed MIA formation *in vitro*.

Supplementary Figure 7 ¹³C NMR spectra of labeled MIAs.

Supplementary Figure 8 Partial ¹H NMR spectrum of the mixture of MIA (**1**) and [²H₆]MIA (**5**).

Supplementary Figure 9 GC-EI-MS analysis of 3-methylindole (**6**) production in NosL-catalyzed *in vitro* conversion.

Supplementary Figure 10 Characterization of glyoxylate-DNP (**8**).

Supplementary Figure 11 Characterization of formaldehyde-DNP (**10**).

Supplementary Figure 12 Plot of the spin density of L-Trp neutral radical (**11**).

Supplementary Figure 13 Structures and relative free energies of the cleavage products of L-Trp neutral radical (**11**).

Supplementary Figure 14 Characterization of Gly-Dansyl (**22**).

Supplementary Figure 15 Characterization of Met-Dansyl (**24**).

Supplementary Figure 16 HPLC analysis of the production of fluorinated MIAs in *E. coli* strains.

Supplementary Figure 17 ^{19}F NMR spectra of fluorinated MIAs.

Supplementary Figure 18 Characterization of 5'-fluoro-NOS (**27**).

Supplementary Figure 19 Spectra of 5'-fluoro-NOS (**27**) for structural elucidation.

2.2 Supplementary Tables

Supplementary table1 Bacteria strains and plasmids used in this study.

Supplementary table2 Primers used in this study.

Supplementary table3 Evaluation of the substrate specificity of NosL in the *nosL*-expressing *E. coli* strain.

Supplementary table4 Assignment of ^1H NMR and ^1H - ^{13}C correlations (HSQC) of 5'-fluoro-NOS (**27**).

Supplementary table5 Minimum inhibitory concentrations (MICs) of NOS and 5'-fluoro-NOS (**27**).

3. Supplementary References

1. Supplementary Methods

1.1. General Materials and Methods

Materials. Biochemicals and media were purchased from Sinopharm Chemical Reagent Co. Ltd. or Oxoid Ltd. unless otherwise stated. Restriction enzymes were from TaKaRa Biotechnology Co. Ltd.. Chemicals, including 5-fluoro-DL-Trp ($\geq 99\%$ purity) and 6-fluoro-DL-Trp (98% purity), were from Sigma-Aldrich Co. Ltd., except L-[$^2\text{H}_8$]-Trp (98% purity), L-[1- ^{13}C]-Trp (99% purity), and L-[3- ^{13}C]-Ser (99% purity), which were purchased from Cambridge Isotope Laboratory Co. Ltd..

DNA Isolation, Manipulation, and Sequencing. DNA isolation and manipulation in *E. coli* were carried out according to the standard methods¹. PCR amplifications were carried out on an Authorized Thermal Cycler (Eppendorf AG 22331 Hamburg, Germany) using either *Taq* DNA polymerase or PfuUltra™ High-Fidelity DNA polymerase (Dalian Takara Biotechnology Co. Ltd., China). Primer synthesis and DNA sequencing were performed at the Shanghai Invitrogen Biotech Co. Ltd. and Chinese National Human Genome Center.

Sequence Analysis. Protein comparison was carried out by available BLAST methods (<http://www.ncbi.nlm.nih.gov/blast/>). Amino acid sequence alignment was performed by the CLUSTALW method, and the DRAWTREE and DRAWGRAM methods, respectively, from BIOLOGYWORKBENCH 3.2 software (<http://workbench.sdsc.edu>).

Compound Analysis. High performance liquid chromatography (HPLC) analysis was carried out on a

JASCO LC-2000 HPLC system (Tokyo, Japan), or on an Agilent™ 1100 HPLC system (Agilent Technologies Inc., USA). Electrospray ionization MS (ESI-MS) was performed on a Thermo Fisher LTQ Fleet ESI-MS spectrometer (Thermo Fisher Scientific Inc., USA). Gas chromatography (GC)-MS analysis was performed on an Agilent 7890A/3973 GC-MS system (Agilent Technologies Inc., USA). ESI-high resolution MS (ESI-HR-MS) analysis was carried out on a Bruker APEXIII 70 Tesla FT-MS system (Bruker Co., Ltd., Germany). NMR data were recorded on Varian Mercury 300 and Varian Unity Inova 600 (Varian Inc., USA), or on Bruker AV400 and Bruker AV500 spectrometers (Bruker Co. Ltd., Germany).

1.2. Gene Cloning and Expression

Constructs for Gene Expression in Escherichia coli BL21 (DE3). A 1.2 kb PCR product containing *nosL* was amplified by PCR using the primer pair NosL-for and NosL-Rev from pSL4001, a pOJ446-based *S. actuosus* genomic library cosmid that contains the nosiheptide (NOS) biosynthetic gene cluster², and then cloned into pSP72 to yield pSL4100. After sequencing to confirm the fidelity, the 1.2 kb EcoRI/HindIII fragment was recovered from pSL4100 and ligated into the same site of pET28a, making the recombinant construct pSL4101 for expressing *nosL* to give the *N*-terminally 6 x His-tagged protein.

Similarly, the flavodoxin-encoding gene *fldA* and the flavodoxin reductase-encoding gene *fpr* were cloned by PCR from *E. coli* BL21(DE3) to constitute the *N*-terminally 6 x His-tagged, natural reduction system: a 0.5 kb EcoRI/SalI product amplified with the primer pair FldA-for and FldA-rev was inserted into pET28a, making the recombinant plasmid pSL4110 for expressing *fldA*; and a 0.75 kb EcoRI/HindIII product amplified with the primer pair Fpr-for and Fpr-rev was inserted into pET28a, making the recombinant plasmid pSL4111 for expressing *fpr*.

Site-Specific Mutagenesis for Expressing Mutant *nosL*. The recombinant plasmid pSL4100 (pSP72 derivative) that contains a 1.2 kb fragment encoding NosL serves as the template. To evaluate the [4Fe-4S] binding potential, PCR amplifications were carried out by using the primer pair NLC95A-for and NLC95A-rev for mutation of C95, the primer pair NLC99A-for and NLC99A-rev for mutation of C99, and the primer pair NLC102A-for and NLC102A-rev for mutation of C102, respectively, to Ala in the characteristic CxxxCxxC motif. To evaluate the *S*-AdoMet binding potential, PCR amplification was performed by using the primer pair NLG142A-for and NLG142A-rev for mutation of the conserved G142 to Ala. After sequencing to confirm the fidelity, the mutant DNA fragments were cloned individually into pET28a, yielding the recombinant constructs for producing NosL mutants (i.e. pSL4103 for C95A, pSL4105 for C99A, pSL4107 for C102A, and pSL4109 for G142A).

1.3. Protein Purification and Characterization

Production and Aerobic Purification of *NosL*, *FldA* and *Fpr*. The constructs pSL4101, pSL4110 and pSL4111 were introduced into *E. coli* BL21 (DE3), yielding the recombinant strains SL4101, SL4110 and SL4111, respectively, for overproduction of NosL, FldA and Fpr. Cells for each protein production were cultured in the Luria-Bertani (LB) medium supplemented with 50-100 µg/mL of kanamycin at 37°C and 250 rpm until the cell density reached 0.6-0.8 at OD_{600 nm}. To induce protein expression, IPTG (0.05-0.1 mM) was added to the cultures, which were further incubated at 25-30°C for 8-12 hr. The soluble fraction for each overproduced protein was loaded onto a Ni-NTA resin (Qiagen, Valencia, USA) column for affinity purification. The purified proteins were dialyzed against cold TSG buffer (50 mM Tris-HCl, 25 mM NaCl, 10% glycerol and 0.02% NaN₃, pH 8.0) overnight at 4°C. The resulting proteins were

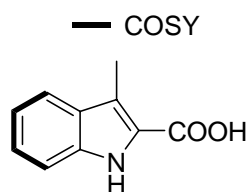
concentrated with an ultracentrifugation filter (Millipore, Billerica, USA) and then stored at -80°C for *in vitro* assays. The purity of proteins was examined by 12% SDS-PAGE analysis, and the concentration was determined by Bradford assay using bovine serum albumin (BSA) as a standard.

Production and Anaerobic Purification of NosL. The recombinant strain SL4101 was cultured in *E. coli* BL21(DE3) and induced by isopropyl- β -D-thiogalactopyranoside (IPTG) for NosL production. The purification then proceeded in an anaerobic glove box (Coy Laboratory Product Inc., USA) with less than 2 ppm of O_2 . The cells were collected from 1 L of the culture broth and resuspended in 20 ml of the lysis buffer (50 mM MOPS, 300 mM NaCl, and 10% glycerol, pH 8.0). In the presence of 2 mg of lysozyme, the suspension was stirred for 1 hr at the room temperature, and broken up by a sonicator (Sonics & Materials, Inc., USA) on ice after adding of 0.1 ml of phenylmethylsulfonyl fluoride (20 mg/ml in isopropyl alcohol). While the cell debris was removed by centrifugation, the supernatant was incubated with 4 ml of Ni-NTA resin pre-equilibrated with the lysis buffer, and then subjected to affinity purification on a column. The purified protein was concentrated with an ultracentrifugation filter to 100 μM and the purity ($>90\%$) was determined by 12% SDS-PAGE analysis.

Characterization of the Reconstituted NosL. Measurement of the absorbance was carried out on a JASCO V-530 UV/Vis spectrophotometer (Tokyo, Japan), in a cuvette sealed with rubber septa to minimize air exposure. The quantification of Fe and S atoms per molecule of the protein was performed in duplicate according to the methods previously described^{3,4}. EPR analysis was carried out on a Bruker EMX plus 10/12 spectrometer system (Bruker Co., Ltd., Germany) at High Magnetic Field Laboratory, Chinese Academy of Sciences, Hefei, China. The reconstituted NosL (100 μM) in the presence of 2 mM sodium

dithionite was loaded into a quartz EPR tube, frozen in liquid nitrogen and then stored in dry ice before recording the spectrum.

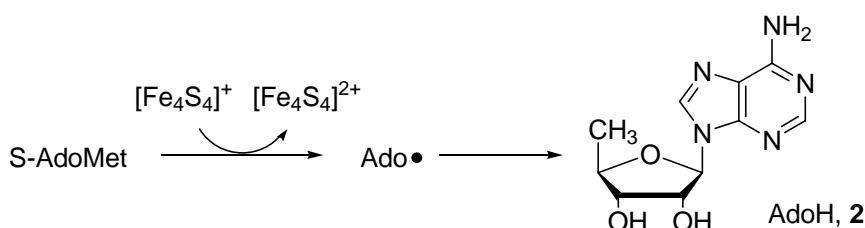
1.4. Determination of the Products, Shunt Products, and Intermediate in NosL-Catalyzed Conversion



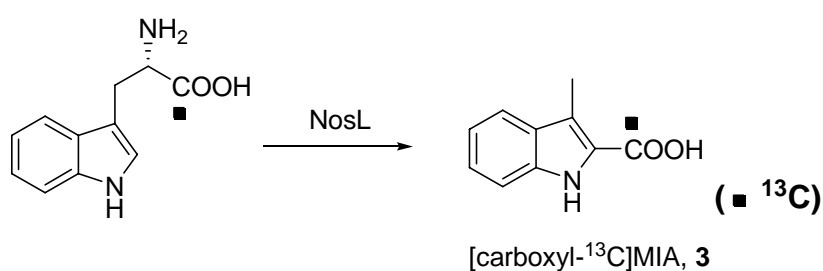
3-methyl-2-indolic acid, MIA, **1**

MIA (Product). HPLC analysis was carried out on an Agilent ZORBAX SB-C18 column (4.6 x 150 mm, product number 993967-902). The column was equilibrated with 85% solvent A (H₂O, 0.1% TFA) and 15% solvent B (CH₃CN, 0.1% TFA), and developed at a flow rate of 1 ml/min and UV detection at 298 nm: 0-3 min, constant 85% A/15% B; 3-6 min, a linear gradient to 60% A/40% B; 6-12 min, constant 60% A/40% B; and 12-20 min, a linear gradient to 45%A/55% B. For isolation, 2 L of the *nosL*-expressing culture broth was centrifuged. The supernatant was adjusted to pH 2.8 with 2M HCl and extracted twice by 500 ml of the mixture of CH₂Cl₂ and n-butanol (with the ratio 4:1), while the precipitate was soaked by 200 ml of tetrahydrofuran (THF) for 2-3 hr before the filtration. Both the organic phases were combined, evaporated to dryness and then re-dissolved in 5 ml of THF. After centrifugation and filtration to remove the precipitate, the product was purified by semi-preparative HPLC on an Agilent ZORBAX SB-C18 column (9.4 x 250 mm, product number 880975-202) that was equilibrated with the solvents A (55%) and B (45%), under the program (0-20 min, constant 55% A/45% B) at a flow rate of 2.2 ml/min. ¹H NMR (400 MHz, d₆-DMSO): δ 11.28 (s, 1H), 7.60 (d, J = 8.02, 1H), 7.37 (d, J = 8.15, 1H), 7.20 (m, 1H), 7.02

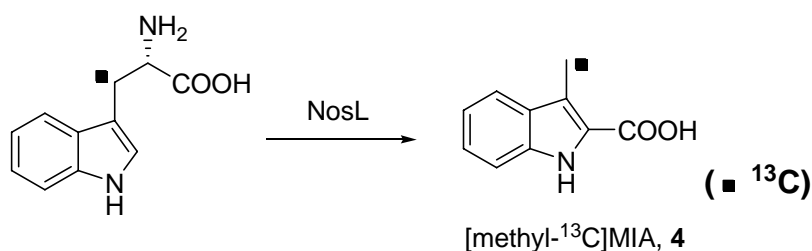
(m, 1H), 2.50 (s, 3H); ^{13}C NMR (100 MHz, d_6 -DMSO): δ 164.0, 135.9, 127.9, 125.1, 124.2, 120.1, 119.0, 116.9, 112.2, 9.7; UV/Vis λ_{max} 230 nm and 298 nm; HR-ESI-MS (m/z): $[\text{M}-\text{H}]^-$ calcd. for $\text{C}_{10}\text{H}_8\text{O}_2\text{N}$, 174.05615; found, 174.05605.



AdoH (Product). AdoH production was measured in NosL-catalyzed *in vitro* conversion, using either L-Trp or L- ^{13}C -Trp as the substrate. HPLC analysis was carried out on an Agilent ZORBAX SB-C18 column (4.6 x 250 mm, product number 880975-902). The column was equilibrated with 2% solvent A (H_2O , 0.1% TFA) and 98% solvent B (CH_3CN , 0.1% TFA), and developed at a flow rate of 1.0 ml/min and UV detection at 260 nm: 0-3 min, constant 98% A/2% B; and 3-20 min, a linear gradient to 80% A/20% B. HR-ESI-MS (m/z): $[\text{M}+\text{H}]^+$ calcd. for $\text{C}_{10}\text{H}_{14}\text{N}_5\text{O}_3$, 252.10967; found 252.10983.

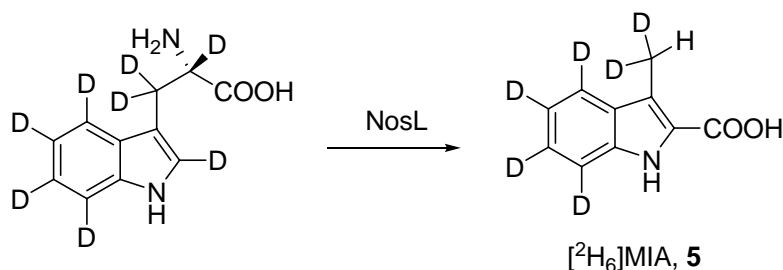


[Carboxyl- ^{13}C]MIA (Product). Feeding of L- ^{13}C -Trp was conducted as described in Methods of the text. The isolation, purification and analysis were performed in the same ways to those for MIA. The ^1H NMR (400 MHz, d_6 -DMSO) spectrum was identical to that of MIA. The enriched signal at δ 164.0 in ^{13}C NMR (400 MHz, d_6 -DMSO) spectrum was found.

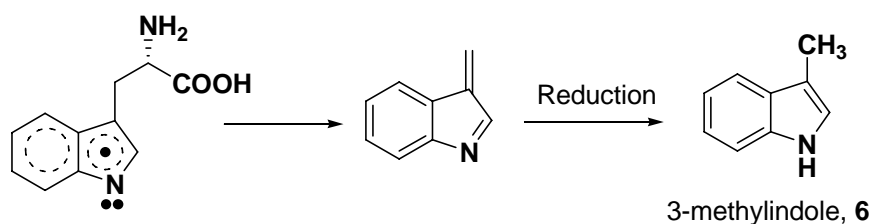


[Methyl-¹³C]MIA (Product). Feeding of L-[3-¹³C]Trp was conducted as described in Methods of the text.

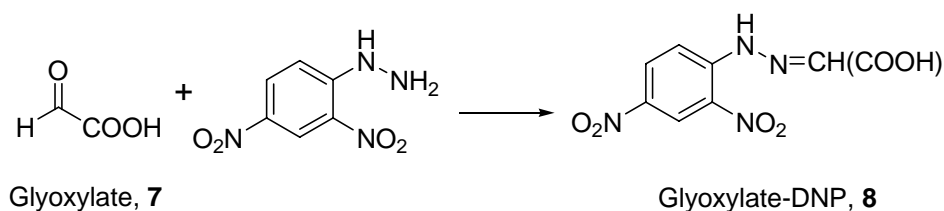
The isolation, purification and analysis were performed in the same ways to those for MIA. The ¹H NMR (400 MHz, d₆-DMSO) spectrum was identical to that of MIA. The enriched signal at δ 8.83 in ¹³C NMR (400 MHz, d₆-DMSO) spectrum was found.



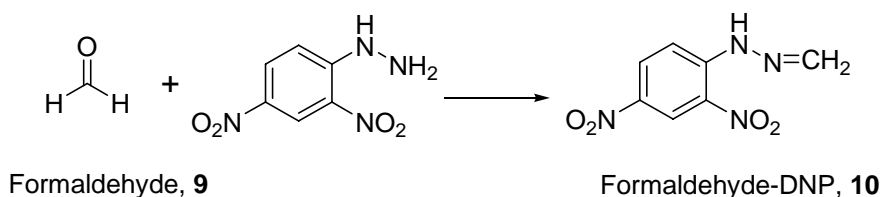
[²H₆]MIA (Product). Feeding of L-[²H₈]Trp was conducted as described in Methods of the text. The isolation, purification and analysis were performed in the same ways to those for MIA. The signal at δ 2.44 (m), 0.04 ppm upfield-shifted from δ 2.48 (s) in ¹H NMR (500 MHz, CD₃OD) spectrum, and the signal at δ 23.4, 0.5 ppm upfield-shifted from δ 23.9 in ¹³C NMR (100MHz, d₈-THF) spectrum, corresponding to CHD₂ relative to CH₃ were found. ¹³C NMR (100 MHz, d₈-THF, for the mixture of **1** and **5**): δ 163.7, 162.1, 137.5, 129.3, 129.2, 125.3, 125.1, 120.9, 119.8, 119.2, 119.1, 116.9, 112.5, 23.9, 23.4; HR-ESI-MS (*m/z*): [M-H]⁻ calcd. for C₁₀H₂D₆O₂N, 180.09371; found, 180.09343.



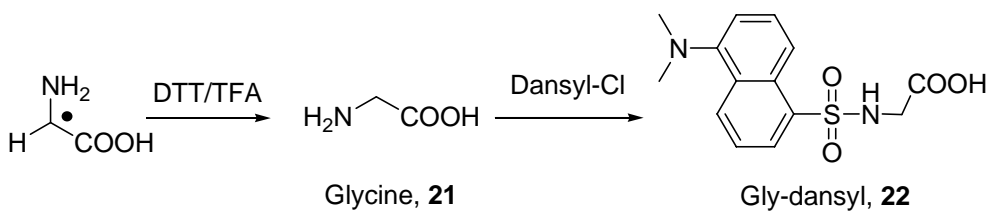
3-Methylindole (Shunt Product). 3-methylindole (**6**) production was measured in NosL-catalyzed *in vitro* conversion, using L-Trp as the substrate. HPLC analysis was performed according to the method identical to that for MIA examination. GC-MS analysis was carried on a PE-Wax (30 m x 0.25 mm x 0.25 μ m) column. The column was initially maintained at 40°C and developed at a flow rate of 1.0 ml/min using helium as a carrier gas: 40°C for 4 min, then increased to 240°C at a speed of 20°C/min, and 240°C for further 6 min. **6** was eluted at a retention time of 9.39 min. The EI-MS were shown as 131.0 (M^+ , 56), 130.0 (100), 103.0 (7.8), 89.0 (2.2), 77.1 (15), 64.9 (8.3), 52.0 (6.7), 44.0 (11), 32.1 (4.4). The analysis of authentic **6** was performed under the same condition. The EI-MS were shown as 131.0 (M^+ , 62), 130.0 (100), 103 (10), 89.0 (1.4), 77.0 (15), 65.0 (7.6), 51.0 (6.8), 39.0 (2.0), 27.0 (1.2).



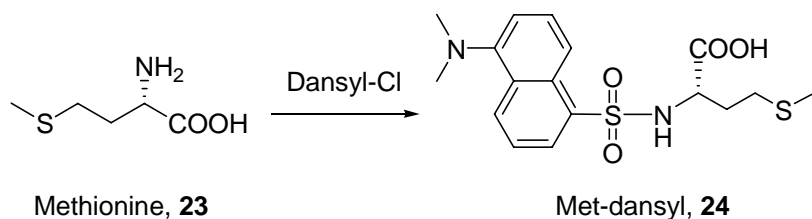
Glyoxylate (Shunt Product). Glyoxylate (**7**) production was measured by derivatization with DNP in NosL-catalyzed *in vitro* conversion, using L-Trp as the substrate. HPLC-MS analysis was carried out on an Agilent ZORBAX SB-C18 column (4.6 x 250 mm, product number 880975-902). The column was equilibrated with 90% solvent A (H₂O, 0.1% formic acid) and 10% solvent B (CH₃CN, 0.1% TFA), and developed at a flow rate of 1.0 ml/min and UV detection at 350 nm: 0-3 min, constant 90% A/10% B; 3-6 min, a linear gradient to 70% A/30% B; 6-12 min, constant 70% A/30% B; and 12-20 min, a linear gradient to 40% A/60% B. For 2-(2,4-dinitrophenyl) hydrazoneacetate (Glyoxylate-DNP, **8**), UV/Vis λ_{\max} 222 nm, 272 nm, and 360nm; ESI-MS (m/z): [$M-H$]⁻ calcd. for C₈H₅N₄O₆, 253.0; found, 253.3.



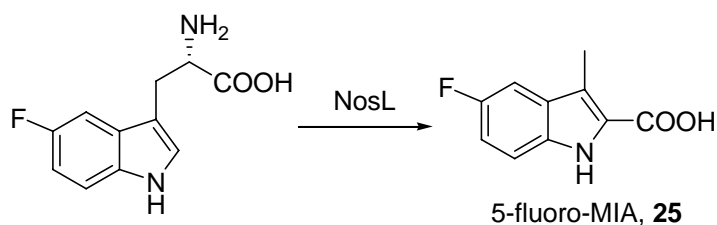
Formaldehyde (Product). Formaldehyde (**9**) production was measured by derivatization with DNP in NosL-catalyzed *in vitro* conversion, using L-Trp as the substrate. HPLC-MS analysis was performed according to the method identical to that for glyoxylate examination. For 1-(2,4)-dinitrophenyl)-2-methylene hydrazine (Formaldehyde-DNP, **10**), UV/Vis λ_{\max} 210 nm, 262 nm, and 346 nm; ESI-MS (m/z): $[M-H]^-$ calcd. for $C_7H_5N_4O_4$, 209.0; found 209.2.



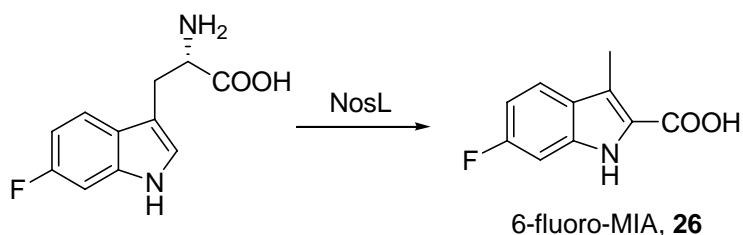
Glycine (putative derivative of glycyl radical). The examination of glycine (**21**) was carried out by quenching NosL-catalyzed *in vitro* conversion at 10 sec, before derivatization with dansyl chloride. HPLC-MS analysis was carried out on an Agilent ZORBAX SB-C18 column (4.6 x 150 mm, product number 993967-902). The column was equilibrated with 90% solvent A (H_2O , 0.1% Formic acid) and 10% solvent B (CH_3CN , 0.1% TFA), and developed at a flow rate of 1.0 ml/min and UV detection at 285 nm: 0-3 min, constant 90% A/10% B; 3-6 min, a linear gradient to 70% A/30% B; 6-12 min, constant 70% A/30% B; and 12-20 min, a linear gradient to 50% A/50% B. For Gly-dansyl (**22**), UV/Vis λ_{\max} 224 nm, 285 nm, and 322 nm; ESI-MS (m/z): $[M+H]^+$ calcd. for $C_{14}H_{17}N_2O_4S$, 309.1; found 309.4.



L-Met (Product). L-Methionine (**23**) production was measured by derivatization with dansyl chloride in NosL-catalyzed *in vitro* conversion as described above for glycine examination. HPLC-MS analysis was performed according to the method identical to that for Gly-dansyl detection. For Met-dansyl (**24**), UV/Vis λ_{\max} 224 nm, 285 nm, and 322 nm; ESI-MS (m/z): $[M+H]^+$ calcd. for $C_{17}H_{23}N_2O_4S_2$, 382.1; found 383.2.



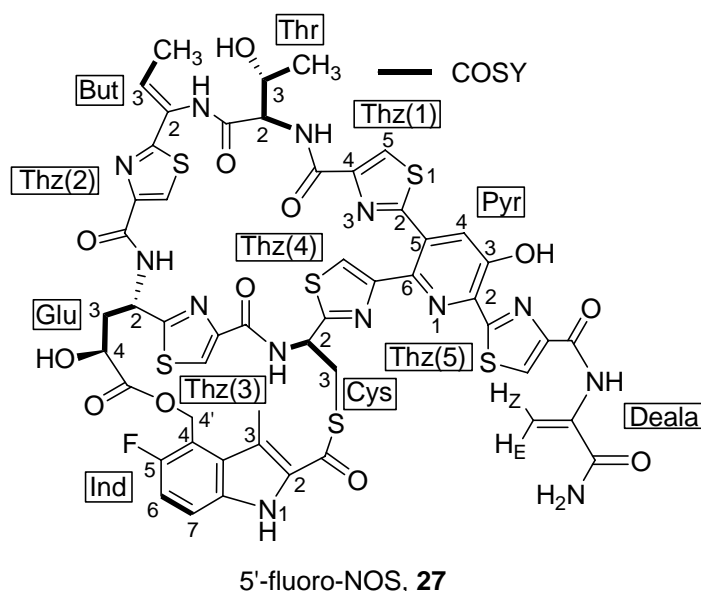
5-Fluoro-MIA (Product). Feeding of 5-fluoro-DL-Trp was conducted as described in Methods of the text. The isolation, purification and analysis were performed in the same ways to those for MIA. 1H NMR (400 MHz, d_6 -DMSO): δ 11.21 (s, 1H), 7.30 (m, 2H), 6.99 (m, 1H), 2.46 (s, 3H); ^{13}C NMR (100MHz, d_6 -DMSO): δ 156.7, 154.4, 131.1, 127.1, 117.0, 112.2, 112.1, 111.5, 111.1, 103.1, 102.8, 17.4; ^{19}F NMR (376 MHz, d_6 -DMSO): δ -119.6; UV/Vis λ_{\max} 227 nm, 242 nm, and 302 nm; HR-ESI-MS (m/z): $[M-H]^-$ calcd. for $C_{10}H_7FO_2N$, 192.04663; found, 192.04637.



6-Fluoro-MIA (Product). Feeding of 6-fluoro-DL-Trp was conducted as described in Methods of the text.

The isolation, purification and analysis were performed in the same ways to those for MIA. ^1H NMR (400 MHz, d_8 -THF) δ 10.56 (s, 1H), δ 7.47 (dd, $J = 8.8, 5.4$, 1H), 6.92 (dd, $J = 9.8, 2.2$, 1H), 6.72 (m, 1H), 2.45 (s, 3H); ^{13}C NMR (100 MHz, d_8 -THF): δ 163.6, 161.4, 137.5, 137.3, 126.2, 125.8, 122.4, 122.3, 119.6, 116.9, 23.5; ^{19}F NMR (282 MHz, CD_3OD) δ -120.2; UV/Vis λ_{max} 227 nm, 242 nm, and 302 nm; HR-ESI-MS (m/z): $[\text{M}-\text{H}]^-$ calcd. for $\text{C}_{10}\text{H}_7\text{FO}_2\text{N}$, 192.04663; found, 192.04624.

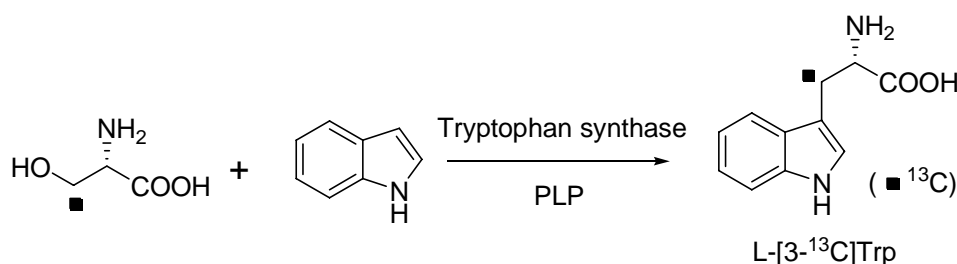
1.5. Determination of 5'-fluoro-NOS



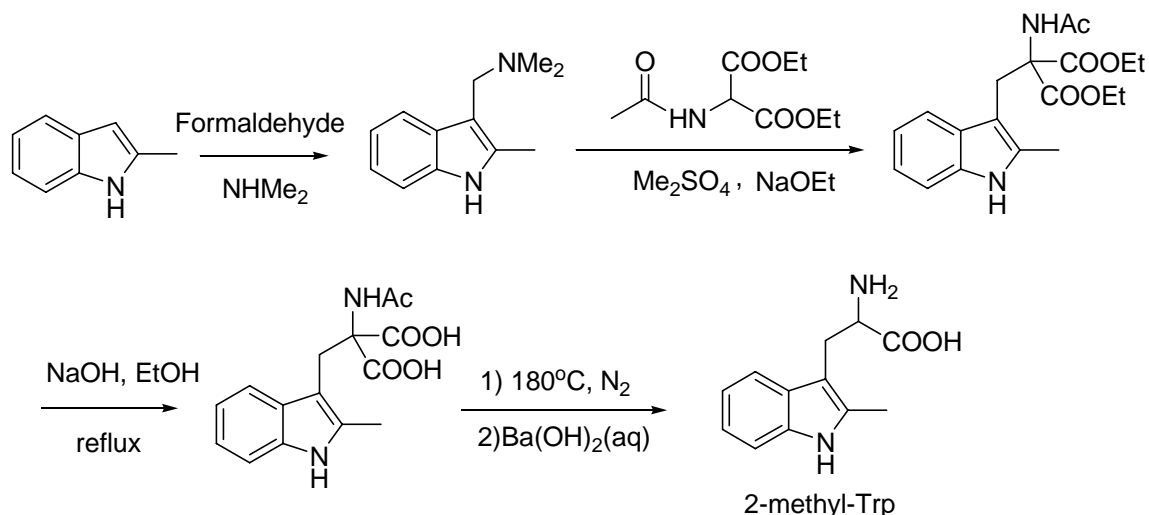
5'-fluoro-NOS. The fermentation, isolation and analysis were carried out similar to the methods described previously⁵. For 5'-fluoro-NOS (**27**) production, 5-fluoro-DL-Trp was supplemented to the fermentation culture of *S. actuosus* at 28-32 hr and 52-56 hr, respectively, to a final concentration of 0.2 mM. ^1H NMR (600 MHz, d_8 -THF): δ 10.76 (br, 1H), 10.19 (s, br, 1H), 9.81 (s, 1H), 8.76 (s, 1H), 8.63 (s, br, 1H), 8.32 (s, 1H), 8.13 (s, 1H), 7.93 (s, 1H), 7.79 (m, 1H), 7.77 (s, 1H), 7.70 (s, 1H), 7.43 (d, $J = 9.50$, 2H), 7.09 (m, 1H), 6.89 (br, 1H), 6.52 E (s, 1H), 6.33 (q, $J = 7.00$, 1H), 5.86 (m, 1H), 5.69 (t, $J = 10.50$, 1H), 5.45 Z (s, 1H), 5.42 (m, 2H), 4.32 (m, 1H), 3.89 (m, 2H), 2.09 (s, 3H), 1.67 (d, $J = 6.00$, 3H), 0.75 (d, $J = 6.50$, 3H);

^{13}C NMR (150 MHz, d_8 -THF): δ 177.9, 173.9, 171.7, 171.4, 170.7, 168.2, 167.8, 166.4, 165.9, 161.8, 160.7, 160.4, 159.0, 158.1, 156.6, 155.9, 152.9, 152.9, 152.0, 151.7, 151.5, 149.8, 145.5, 135.6, 135.5, 135.4, 132.9, 131.9, 130.5, 129.0, 128.1, 127.2, 126.9, 126.8, 125.7, 125.1, 121.5, 120.0, 117.2, 115.6, 68.0, 64.6, 58.4, 58.3, 50.9, 46.8, 35.3, 29.9, 23.2, 21.5, 14.7; ^{19}F NMR (376 MHz, d_6 -DMSO): δ -126.5; UV/Vis λ_{max} 222 nm and 357 nm; HR-ESI-MS (m/z): $[\text{M}-\text{H}]^-$ calcd. for $\text{C}_{51}\text{H}_{41}\text{FN}_{13}\text{O}_{12}$, 1238.13114; found 1238.12959; Tandem ESI-MS (Positive ion scanning): 1239.9, 1220.0, 1196.0, 1149.4, 1116.0, 1035.1, 956.7, 904.7. Assignment of the ^1H NMR and ^1H - ^{13}C COSY correlations (HSQC) of 5'-fluoro-NOS was summarized in Supplementary Table S4.

1.6. Synthesis



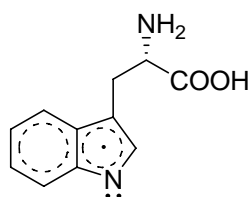
L-[3- ^{13}C]Trp. Using indole and L-[3- ^{13}C]Ser as the substrates, L-[3- ^{13}C]Trp was synthesized enzymatically by tryptophan synthase according to the method described previously⁶. ^1H NMR (400MHz, D_2O): δ 7.62 (d, $J = 8.0$, 1H), 7.43 (d, $J = 8.0$, 1H), 7.18 (t, $J = 8.0$, 1H). 7.10 (t, $J = 7.6$, 1H), 3.94 (dd, $J = 8.0$, 4.4, 1H), 3.37 (dd, $J = 15.2$, 4.4, 1H), 3.19 (dd, $J = 15.2$, 4.4, 1H); ^{13}C NMR (100MHz, D_2O): δ 26.3 (enriched), ESI-MS (m/z): $[\text{M}+\text{H}]^+$ calcd. for $\text{C}_{10}^{13}\text{CH}_{13}\text{N}_2\text{O}_2$, 206.1; found 206.1.



2-Methyl-Trp. A previously reported method⁷ was utilized to synthesize 2-methyl-Trp, giving 300 mg of the product as a white powder (approximately 30% for the overall yield). ¹H NMR (400 MHz, d₆-DMSO): δ 8.17 (s, 1H), 7.43 (d, J = 8.0, 1H), 7.24 (d, J = 8.0, 1H), 6.99 (m, 1H), 6.93 (m, 1H), 3.96 (dd, J = 8.0 Hz, 5.2 Hz, 1H), 3.16 (dd, J = 5.2 Hz, 5.2 Hz, 2H), 2.30 (s, 3H); ¹³C NMR (100 MHz, d₆-DMSO): δ 171.2, 134.7, 132.1, 128.5, 120.7, 118.8, 117.6, 110.9, 105.2, 53.2, 26.2, 11.9; ESI-MS (*m/z*): [M+H]⁺ calcd. for C₁₂H₁₅N₂O₂, 219.1, found 219.1.

1.7. Theoretical Calculations

Density functional theory (DFT)^{8,9} studies have been performed with the Gaussian03 program¹⁰ using the unrestricted B3LYP^{11,12} method and the 6-311+G** basis set. The optimized structures were all checked with harmonic vibration frequency calculations. The solvent effect was estimated with IEFPCM^{13,14} (UAHF atomic radii) method in water ($\epsilon=78.39$) using the gas-phase optimized structures. Calculated total energies and geometrical coordinates of the possible intermediates are listed below.



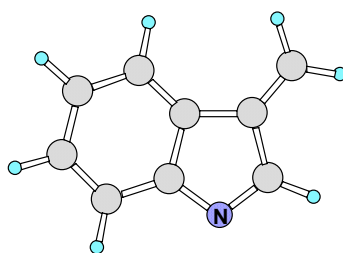
L-trp neutral radical, **11**

L-Trp neutral radical (11) in Fig. 3, and Supplementary Figs. 12 and 13.

SCF Done: E(UB3LYP) = -685.908051360 Hartree
 <S**2> = 0.7671 S = 0.5085

Zero-point correction =	0.204958 (Hartree/Particle)
Thermal correction to Energy =	0.217770
Thermal correction to Enthalpy =	0.218714
Thermal correction to Gibbs Free Energy =	0.162813
Sum of electronic and zero-point Energies =	-685.703093
Sum of electronic and thermal Energies =	-685.690282
Sum of electronic and thermal Enthalpies =	-685.689338
Sum of electronic and thermal Free Energies =	-685.745238
Sum of electronic and thermal Free Energies =	-685.745238

C,0,-0.933016951,2.1721841811,-0.3441489279
 C,0,-0.2977887731,0.8861110344,-0.530664048
 N,0,-2.1959157246,2.0863556905,0.0007700678
 H,0,-0.4465509185,3.1282936051,-0.4854860108
 C,0,1.1151209861,0.5991202677,-0.9156869827
 H,0,1.7680607059,1.4160551608,-0.5947190635
 H,0,1.4429986278,-0.3089270357,-0.3986437783
 C,0,1.3299079138,0.3513916047,-2.4387387576
 C,0,1.3759747707,1.6771518864,-3.2313662144
 O,0,2.1012699982,1.6076832148,-4.3574825493
 O,0,0.7991792474,2.6746380966,-2.8910854647
 N,0,2.5124413278,-0.448014996,-2.7878112363
 H,0,3.3187233094,-0.2006300939,-2.2209579989
 H,0,2.3476237681,-1.4416481002,-2.6770953407
 H,0,2.5258611655,0.7243545391,-4.351826162
 H,0,0.4593015576,-0.1859235508,-2.8295230745
 C,0,-1.3951507985,-1.4672616806,-0.2459867913
 C,0,-1.330923434,-0.0715289651,-0.2628742354
 C,0,-2.6127163505,-2.0776620316,0.0802436865
 H,0,-0.5262078671,-2.0773147871,-0.4726240962
 C,0,-2.4822743066,0.7039512313,0.0576390762
 C,0,-3.7347968658,-1.3064122039,0.3858115719
 H,0,-2.684496418,-3.1588575249,0.0980263273
 C,0,-3.6799898883,0.1019743431,0.3802834417
 H,0,-4.6672118746,-1.7997741994,0.6360044499
 H,0,-4.5507482378,0.6993609734,0.6233904513



12

12 in Fig. 3 and Supplementary Fig. 13.

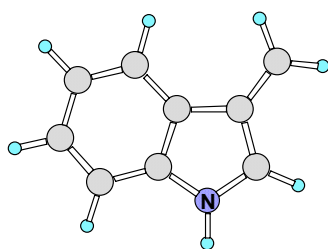
SCF Done: E(UB3LYP) = -401.690159730 Hartree
 <S**2> = 0.7650 S = 0.5075

Zero-point correction =	0.132151 (Hartree/Particle)
Thermal correction to Energy =	0.139663
Thermal correction to Enthalpy =	0.140607
Thermal correction to Gibbs Free Energy =	0.099531
Sum of electronic and zero-point Energies =	-401.558009
Sum of electronic and thermal Energies =	-401.550497
Sum of electronic and thermal Enthalpies =	-401.549553
Sum of electronic and thermal Free Energies =	-401.590629

(Unpolarized solute)-Solvent	(kcal/mol) =	-48.48
(Polarized solute)-Solvent	(kcal/mol) =	-49.69
Solute polarization	(kcal/mol) =	0.67
Total electrostatic	(kcal/mol) =	-49.02

Cavitation energy	(kcal/mol) =	18.52
Dispersion energy	(kcal/mol) =	-18.88
Repulsion energy	(kcal/mol) =	3.20
Total non electrostatic	(kcal/mol) =	2.85
DeltaG (solv)	(kcal/mol) =	-46.18

C,0,-0.1898097223,0.4859838643,0.0000093344
C,0,0.2632491434,-0.8961987237,0.0000052607
C,0,1.6447592294,-1.2336358999,-0.0000011357
C,0,2.5443812786,-0.1971258278,-0.0000027004
C,0,2.0953072317,1.1567786068,0.0000007616
C,0,0.7242201841,1.5070357696,0.0000057741
C,0,-1.6554500139,0.3873828899,0.0000077069
C,0,-1.8866297637,-1.0542049507,0.0000454723
H,0,1.9455273302,-2.2739597454,-0.0000061856
H,0,3.6096455289,-0.3917870776,-0.0000086504
H,0,2.8375470971,1.9473508502,-0.0000019762
H,0,0.4343186928,2.5508413733,0.0000063022
H,0,-2.8587936319,-1.5355989051,0.0000262201
C,0,-2.6058891871,1.3392335115,-0.0000085907
H,0,-3.6578774318,1.0762131669,-0.000001142
H,0,-2.3644629413,2.3961504862,-0.0000181611
N,0,-0.7716060243,-1.7771473885,0.0000037098



16

16 in Fig. 3 and Supplementary Fig. 13.

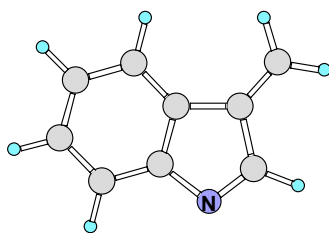
SCF Done: E(UB3LYP) = -402.592158224 Hartree
 <S**2>= 0.7712 S= 0.5105

Zero-point correction =	0.143185 (Hartree/Particle)
Thermal correction to Energy =	0.150980
Thermal correction to Enthalpy =	0.151924
Thermal correction to Gibbs Free Energy =	0.110620
Sum of electronic and zero-point Energies =	-402.448973
Sum of electronic and thermal Energies =	-402.441178
Sum of electronic and thermal Enthalpies =	-402.440234
Sum of electronic and thermal Free Energies =	-402.481538

(Unpolarized solute)-Solvent	(kcal/mol) =	-6.53
(Polarized solute)-Solvent	(kcal/mol) =	-9.04
Solute polarization	(kcal/mol) =	1.39
Total electrostatic	(kcal/mol) =	-7.65

Cavitation energy	(kcal/mol) =	18.38
Dispersion energy	(kcal/mol) =	-19.98
Repulsion energy	(kcal/mol) =	3.72
Total non electrostatic	(kcal/mol) =	2.12
DeltaG (solv)	(kcal/mol) =	-5.53

C,0,0.186206,-0.434721,-0.000029
 C,0,-0.312138,0.888832,-0.0000000435
 C,0,-1.678085,1.171583,0.000031
 C,0,-2.556059,0.093467,0.000036
 C,0,-2.082933,-1.229758,0.000008
 C,0,-0.718664,-1.500041,-0.000024
 C,0,1.648115,-0.36053,-0.000053
 C,0,1.944736,1.012732,-0.00001
 H,0,-2.04522,2.192053,0.000045
 H,0,-3.624334,0.27784,0.000059
 H,0,-2.79351,-2.0482,0.000011
 H,0,-0.36388,-2.524671,-0.000045
 H,0,2.906089,1.501347,0.000009
 C,0,2.555,-1.420507,-0.000054
 H,0,3.62281,-1.24328,0.000862
 H,0,2.217214,-2.447978,-0.000128
 N,0,0.776918,1.74524,-0.000032
 H,0,0.725332,2.749875,-0.000016



14

14 in Fig. 3 and Supplementary Fig. 13.

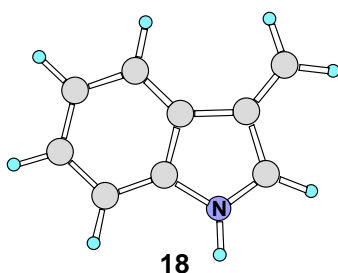
SCF Done: E(UB3LYP) = -401.995104928 Hartree
 <S**2>= 0.0000 S= 0.0000

Zero-point correction =	0.133245 (Hartree/Particle)
Thermal correction to Energy =	0.140435
Thermal correction to Enthalpy =	0.141379
Thermal correction to Gibbs Free Energy =	0.101563
Sum of electronic and zero-point Energies =	-401.861860
Sum of electronic and thermal Energies =	-401.854670
Sum of electronic and thermal Enthalpies =	-401.853726
Sum of electronic and thermal Free Energies =	-401.893542

(Unpolarized solute)-Solvent	(kcal/mol) =	-5.16
(Polarized solute)-Solvent	(kcal/mol) =	-7.57
Solute polarization	(kcal/mol) =	1.37
Total electrostatic	(kcal/mol) =	-6.20

Cavitation energy	(kcal/mol) =	18.49
Dispersion energy	(kcal/mol) =	-18.87
Repulsion energy	(kcal/mol) =	3.20
Total non electrostatic	(kcal/mol) =	2.81
DeltaG (solv)	(kcal/mol) =	-3.39

C,0,-0.174614,0.446995,-0.000004
C,0,0.265303,-0.892644,-0.000006
C,0,1.614618,-1.210752,-0.000004
C,0,2.533747,-0.155798,0.000004
C,0,2.105747,1.174398,0.000009
C,0,0.742218,1.489321,0.000005
C,0,-1.643648,0.370741,-0.000015
C,0,-1.899921,-1.089007,0.000035
H,0,1.937048,-2.245075,-0.000009
H,0,3.59601,-0.372961,0.000007
H,0,2.839408,1.972375,0.000014
H,0,0.421144,2.525669,0.000007
H,0,-2.888571,-1.536945,0.000055
C,0,-2.573057,1.335468,-0.000009
H,0,-3.630068,1.093257,0.000065
H,0,-2.310193,2.387423,-0.000069
N,0,-0.826734,-1.805153,-0.000023



18 in Fig. 3 and Supplementary Fig. 13.

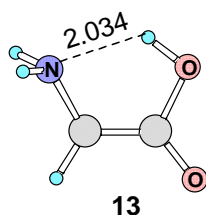
SCF Done: E(UB3LYP) = -402.367550234 Hartree
 <S**2>= 0.0000 S= 0.0000

Zero-point correction=	0.146993 (Hartree/Particle)
Thermal correction to Energy =	0.154287
Thermal correction to Enthalpy =	0.155231
Thermal correction to Gibbs Free Energy =	0.115256
Sum of electronic and zero-point Energies =	-402.220557
Sum of electronic and thermal Energies =	-402.213263
Sum of electronic and thermal Enthalpies =	-402.212319
Sum of electronic and thermal Free Energies =	-402.252294

(Unpolarized solute)-Solvent	(kcal/mol) = -50.83
(Polarized solute)-Solvent	(kcal/mol) = -54.37
Solute polarization	(kcal/mol) = 1.99
Total electrostatic	(kcal/mol) = -52.38

Cavitation energy	(kcal/mol) = 18.71
Dispersion energy	(kcal/mol) = -19.29
Repulsion energy	(kcal/mol) = 3.29
Total non electrostatic	(kcal/mol) = 2.71
DeltaG (solv)	(kcal/mol) = -49.66

C,0,0.1591436006,-0.4813672834,0.0001059319
 C,0,-0.3195195572,0.8387994358,0.0000589008
 C,0,-1.6633730425,1.1724448575,-0.0000028316
 C,0,-2.5631675737,0.1048880171,-0.0000777937
 C,0,-2.1151759988,-1.2204994617,-0.000066955
 C,0,-0.7528828942,-1.5308529587,0.0000219188
 C,0,1.6281982831,-0.4023959147,0.000392235
 C,0,1.9343571454,1.0159562473,-0.0000991914
 H,0,-2.0069107426,2.1997647415,-0.0000091404
 H,0,-3.6265972853,0.3089480873,-0.0001339042
 H,0,-2.8414096549,-2.0238971494,-0.0000966938
 H,0,-0.4278491238,-2.5641753999,0.000082268
 H,0,2.9034886391,1.4954701332,-0.0001980704
 C,0,2.5754784595,-1.3634713879,0.0006287788
 H,0,3.6305946093,-1.1145578749,-0.0001145629
 H,0,2.3183161504,-2.416421025,-0.0001179066
 N,0,0.8137896703,1.6953660022,0.0001321287
 H,0,0.7611163153,2.7092839337,0.0001648444



13 in Fig. 3 and Supplementary Fig. 13.

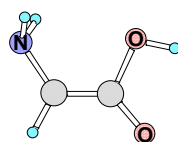
SCF Done: E(UB3LYP) = -283.929206602 Hartree
 <S**2>= 0.0000 S= 0.0000

Zero-point correction =	0.065228 (Hartree/Particle)
Thermal correction to Energy =	0.070478
Thermal correction to Enthalpy =	0.071422
Thermal correction to Gibbs Free Energy =	0.037162
Sum of electronic and zero-point Energies =	-283.863978
Sum of electronic and thermal Energies =	-283.858729
Sum of electronic and thermal Enthalpies =	-283.857785
Sum of electronic and thermal Free Energies =	-283.892045

(Unpolarized solute)-Solvent	(kcal/mol) = -66.08
(Polarized solute)-Solvent	(kcal/mol) = -76.06
Solute polarization	(kcal/mol) = 5.58
Total electrostatic	(kcal/mol) = -70.49

Cavitation energy	(kcal/mol) = 10.62
Dispersion energy	(kcal/mol) = -14.77
Repulsion energy	(kcal/mol) = 5.11
Total non electrostatic	(kcal/mol) = 0.97
DeltaG (solv)	(kcal/mol) = -69.52

C,0,-0.61947417,-0.660999671,0.101735321
 C,0,0.65790704,-0.1505760575,-0.1250431682
 O,0,0.6986451047,1.254284907,-0.3511107847
 O,0,1.7507733813,-0.7451608196,-0.1566530774
 N,0,-1.7676258851,0.2346900284,0.0930945148
 H,0,-2.4518728369,0.0193594645,-0.6285911807
 H,0,-0.2357198954,1.5175472275,-0.2854875214
 H,0,-0.7496481191,-1.7230982982,0.2846141841
 H,0,-2.2662756196,0.272835515,0.9793057125



13-2 in Supplementary Fig. 13.

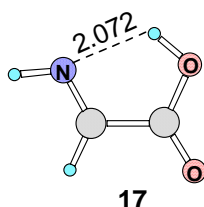
SCF Done: E(UB3LYP) = -283.929283042 Hartree
 <S**2>= 0.0000 S= 0.0000

Zero-point correction =	0.064752 (Hartree/Particle)
Thermal correction to Energy =	0.070417
Thermal correction to Enthalpy =	0.071361
Thermal correction to Gibbs Free Energy =	0.036248
Sum of electronic and zero-point Energies =	-283.864532
Sum of electronic and thermal Energies =	-283.858866
Sum of electronic and thermal Enthalpies =	-283.857922
Sum of electronic and thermal Free Energies =	-283.893035

(Unpolarized solute)-Solvent	(kcal/mol) =	-64.88
(Polarized solute)-Solvent	(kcal/mol) =	-70.32
Solute polarization	(kcal/mol) =	2.90
Total electrostatic	(kcal/mol) =	-67.42

Cavitation energy	(kcal/mol) =	10.84
Dispersion energy	(kcal/mol) =	-14.10
Repulsion energy	(kcal/mol) =	4.37
Total non electrostatic	(kcal/mol) =	1.11
DeltaG (solv)	(kcal/mol) =	-66.30

C,0,-0.7273886991,-0.7734306525,-0.1420939613
 C,0,0.5034236212,-0.180283003,0.0191487639
 O,0,0.4393674853,1.2397391341,0.2733128801
 O,0,1.669364434,-0.654751606,-0.0154487447
 N,0,-1.9971165261,-0.0670101486,-0.0698502868
 H,0,-2.1009541667,0.3967493541,0.8298826485
 H,0,1.3775392798,1.4503598061,0.3539659937
 H,0,-0.7674093649,-1.8382644964,-0.3367653365
 H,0,-2.0319850636,0.6829986122,-0.7565939569



17 in Fig. 3 and Supplementary Fig. 13.

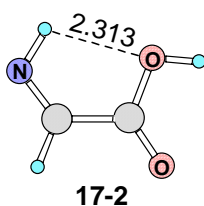
SCF Done: E(UB3LYP) = -283.298388254 Hartree
 <S**2>= 0.0000 S= 0.0000

Zero-point correction =	0.056175 (Hartree/Particle)
Thermal correction to Energy =	0.060868
Thermal correction to Enthalpy =	0.061812
Thermal correction to Gibbs Free Energy =	0.028539
Sum of electronic and zero-point Energies =	-283.242214
Sum of electronic and thermal Energies =	-283.237520
Sum of electronic and thermal Enthalpies =	-283.236576
Sum of electronic and thermal Free Energies =	-283.269849

(Unpolarized solute)-Solvent	(kcal/mol) =	-9.86
(Polarized solute)-Solvent	(kcal/mol) =	-13.75
Solute polarization	(kcal/mol) =	2.14
Total electrostatic	(kcal/mol) =	-11.61

Cavitation energy	(kcal/mol) =	10.82
Dispersion energy	(kcal/mol) =	-12.19
Repulsion energy	(kcal/mol) =	2.85
Total non electrostatic	(kcal/mol) =	1.48
DeltaG (solv)	(kcal/mol) =	-10.13

C,0,0.7989,-0.665506,0.000239
 C,0,-0.59363,-0.070684,0.000058
 O,0,-0.618359,1.267181,0.000012
 O,0,-1.579805,-0.757751,-0.000126
 N,0,1.788185,0.125294,-0.000158
 H,0,2.689472,-0.353127,-0.000282
 H,0,0.308135,1.574842,0.000311
 H,0,0.838789,-1.757078,0.000205



17-2 in Supplementary Fig. 13.

SCF Done: E(UB3LYP) = -283.296678340 Hartree
 <S**2>= 0.0000 S= 0.0000

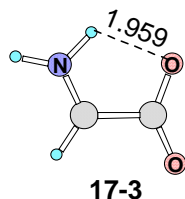
Zero-point correction =	0.055981 (Hartree/Particle)
Thermal correction to Energy =	0.060877
Thermal correction to Enthalpy =	0.061822
Thermal correction to Gibbs Free Energy =	0.027993
Sum of electronic and zero-point Energies =	-283.240698
Sum of electronic and thermal Energies =	-283.235801
Sum of electronic and thermal Enthalpies =	-283.234857
Sum of electronic and thermal Free Energies =	-283.268686

(Unpolarized solute)-Solvent	(kcal/mol) =	-10.48
(Polarized solute)-Solvent	(kcal/mol) =	-13.46
Solute polarization	(kcal/mol) =	1.60
Total electrostatic	(kcal/mol) =	-11.85

Cavitation energy	(kcal/mol) =	10.89
Dispersion energy	(kcal/mol) =	-12.17
Repulsion energy	(kcal/mol) =	2.81
Total non electrostatic	(kcal/mol) =	1.53
DeltaG (solv)	(kcal/mol) =	-10.33

C,0,0.882783,-0.63262,-0.000032
 C,0,-0.534449,-0.116816,-0.000053
 O,0,-0.595865,1.232966,-0.000027
 O,0,-1.501082,-0.834346,0.000033
 N,0,1.937,0.067457,0.000046
 H,0,1.711307,1.066527,-0.000023
 H,0,-1.529977,1.489603,0.000186

H,0,0.945249,-1.72067,-0.00003



17-3 in Supplementary Fig. 13.

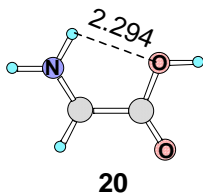
SCF Done: E(UB3LYP) = -283.270209265 Hartree
<S**2>= 0.0000 S= 0.0000

Zero-point correction =	0.054988 (Hartree/Particle)
Thermal correction to Energy =	0.059937
Thermal correction to Enthalpy =	0.060881
Thermal correction to Gibbs Free Energy =	0.026798
Sum of electronic and zero-point Energies =	-283.215222
Sum of electronic and thermal Energies =	-283.210272
Sum of electronic and thermal Enthalpies =	-283.209328
Sum of electronic and thermal Free Energies =	-283.243411

(Unpolarized solute)-Solvent	(kcal/mol) =	-21.77
(Polarized solute)-Solvent	(kcal/mol) =	-33.31
Solute polarization	(kcal/mol) =	6.33
Total electrostatic	(kcal/mol) =	-26.99

Cavitation energy	(kcal/mol) =	10.58
Dispersion energy	(kcal/mol) =	-12.36
Repulsion energy	(kcal/mol) =	2.78
Total non electrostatic	(kcal/mol) =	1.00
DeltaG (solv)	(kcal/mol) =	-25.99

C,0,-0.0699224293,0.0002080579,-0.0014375773
C,0,0.0879571289,-0.0000168983,1.5630977977
O,0,1.2908690686,-0.0004257088,1.8832011788
O,0,-0.9874248062,0.0002655281,2.1608190562
N,0,1.03532063,0.0003014472,-0.647031083
H,0,1.1308634998,0.0002899257,-1.6563639899
H,0,1.8460669643,0.000659978,0.0043667874
H,0,-1.023442291,0.0001001438,-0.5235636245



20 in Fig. 3 and Supplementary Fig. 13.

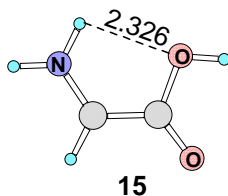
SCF Done: E(UB3LYP) = -283.629755457 Hartree
<S**2>= 0.0000 S= 0.0000

Zero-point correction =	0.069237 (Hartree/Particle)
Thermal correction to Energy =	0.074324
Thermal correction to Enthalpy =	0.075268
Thermal correction to Gibbs Free Energy =	0.040940
Sum of electronic and zero-point Energies =	-283.560519
Sum of electronic and thermal Energies =	-283.555431
Sum of electronic and thermal Enthalpies =	-283.554487
Sum of electronic and thermal Free Energies =	-283.588816

(Unpolarized solute)-Solvent	(kcal/mol) =	-74.36
(Polarized solute)-Solvent	(kcal/mol) =	-79.48
Solute polarization	(kcal/mol) =	2.80
Total electrostatic	(kcal/mol) =	-76.68

Cavitation energy	(kcal/mol) =	10.95
Dispersion energy	(kcal/mol) =	-13.22
Repulsion energy	(kcal/mol) =	3.28
Total non electrostatic	(kcal/mol) =	1.01
DeltaG (solv)	(kcal/mol) =	-75.67

C,0,0.7713026157,-0.667171909,0.0001089839
 C,0,-0.6325948577,-0.0946108073,0.0008524621
 O,0,-0.5872009376,1.2363906451,-0.0001294157
 O,0,-1.5774795223,-0.8219441009,0.000251664
 N,0,1.8053278604,0.0826102062,-0.0000450742
 H,0,2.7518999358,-0.2980908399,-0.0004529758
 H,0,-1.4809352246,1.6225276352,-0.0006540354
 H,0,0.8751875451,-1.7491576044,-0.0001796897
 H,0,1.7024245852,1.1005157749,0.0002920809



15 in Fig. 3 and Supplementary Fig. 13.

SCF Done: E(UB3LYP) = -283.895378775 Hartree
 <S**2>= 0.7554 S= 0.5027

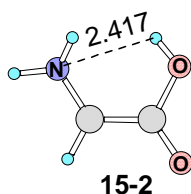
Zero-point correction =	0.066234 (Hartree/Particle)
Thermal correction to Energy =	0.071868
Thermal correction to Enthalpy =	0.072812
Thermal correction to Gibbs Free Energy =	0.037308
Sum of electronic and zero-point Energies =	-283.829145
Sum of electronic and thermal Energies =	-283.823511
Sum of electronic and thermal Enthalpies =	-283.822566
Sum of electronic and thermal Free Energies =	-283.858071

(Unpolarized solute)-Solvent	(kcal/mol) =	-12.12
(Polarized solute)-Solvent	(kcal/mol) =	-16.43
Solute polarization	(kcal/mol) =	2.39

Total electrostatic	(kcal/mol) =	-14.04

Cavitation energy	(kcal/mol) =	11.06
Dispersion energy	(kcal/mol) =	-13.10
Repulsion energy	(kcal/mol) =	3.14
Total non electrostatic	(kcal/mol) =	1.10
DeltaG (solv)	(kcal/mol) =	-12.94

C,0,0.7253807399,-0.6946438526,-0.0369242383
 C,0,-0.5843975941,-0.1331801348,-0.0052180262
 O,0,-0.563157891,1.2485698565,-0.0213830105
 O,0,-1.6336236349,-0.7591154517,0.0365984426
 N,0,1.8442911551,0.0766776216,-0.1190652588
 H,0,2.7564842915,-0.3275449841,0.0079852683
 H,0,-1.4855061092,1.5364082682,0.0061135344
 H,0,0.8319277909,-1.7684123543,-0.0301466548
 H,0,1.7561742518,1.0780160311,-0.0378930567



15-2 in Supplementary Fig. 13.

SCF Done: E(UB3LYP) = -283.879968691 Hartree
 <S**2>= 0.7568 S= 0.5034

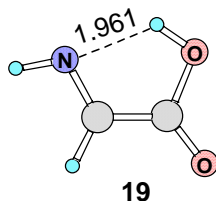
Zero-point correction=	0.066103 (Hartree/Particle)
Thermal correction to Energy =	0.071601
Thermal correction to Enthalpy =	0.072546
Thermal correction to Gibbs Free Energy =	0.037269
Sum of electronic and zero-point Energies =	-283.813866
Sum of electronic and thermal Energies =	-283.808367
Sum of electronic and thermal Enthalpies =	-283.807423
Sum of electronic and thermal Free Energies =	-283.842700

(Unpolarized solute)-Solvent	(kcal/mol) =	-14.47
(Polarized solute)-Solvent	(kcal/mol) =	-22.45
Solute polarization	(kcal/mol) =	4.54
Total electrostatic	(kcal/mol) =	-17.91

Cavitation energy	(kcal/mol) =	11.15
Dispersion energy	(kcal/mol) =	-12.97
Repulsion energy	(kcal/mol) =	3.04
Total non electrostatic	(kcal/mol) =	1.21
DeltaG (solv)	(kcal/mol) =	-16.70

C,0,-0.1044829528,-0.2690923585,-0.0735115014
 C,0,0.0277922105,0.1969459729,1.2794772532
 O,0,1.2983836286,0.5640851431,1.6849026184
 O,0,-0.9065891494,0.3187049014,2.0450943569
 N,0,0.9239106209,-0.2150221921,-0.9882578094
 H,0,1.5605267258,0.5705589166,-0.9446792865

H,0,-1.0306855725,-0.7418655169,-0.3652819984
H,0,1.9614365399,0.0821504612,1.1742336754
H,0,0.715045475,-0.5053437021,-1.9316187049



19 in Fig. 3 and Supplementary Fig. 13.

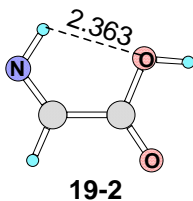
SCF Done: E(UB3LYP) = -283.326424084 Hartree
<S**2>= 0.7553 S= 0.5027

Zero-point correction =	0.053218 (Hartree/Particle)
Thermal correction to Energy =	0.058037
Thermal correction to Enthalpy =	0.058981
Thermal correction to Gibbs Free Energy =	0.025017
Sum of electronic and zero-point Energies =	-283.273206
Sum of electronic and thermal Energies =	-283.268387
Sum of electronic and thermal Enthalpies =	-283.267443
Sum of electronic and thermal Free Energies =	-283.301407

(Unpolarized solute)-Solvent	(kcal/mol) =	-112.81
(Polarized solute)-Solvent	(kcal/mol) =	-150.69
Solute polarization	(kcal/mol) =	21.33
Total electrostatic	(kcal/mol) =	-129.36

Cavitation energy	(kcal/mol) =	10.16
Dispersion energy	(kcal/mol) =	-14.65
Repulsion energy	(kcal/mol) =	9.20
Total non electrostatic	(kcal/mol) =	4.71
DeltaG (solv)	(kcal/mol) =	-124.65

C,0,0.7525559158,-0.6560878622,0.0001711383
C,0,-0.5715494695,-0.1247394601,0.0000344543
O,0,-0.5946585061,1.2685846529,0.0001276825
O,0,-1.6468327765,-0.7452811438,-0.0003199163
N,0,1.811128161,0.1907856968,-0.0003653039
H,0,2.6847723034,-0.3311527416,-0.0003369993
H,0,0.3561339169,1.5050993368,0.0004342736
H,0,0.840137455,-1.7440374789,0.0005136707



19-2 in Supplementary Fig. 13.

SCF Done: E(UB3LYP) = -283.321432627 Hartree

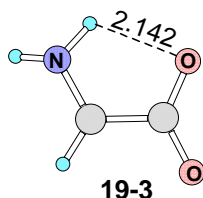
<S**2>= 0.7572 S= 0.5036

Zero-point correction =	0.053149 (Hartree/Particle)
Thermal correction to Energy =	0.058177
Thermal correction to Enthalpy =	0.059121
Thermal correction to Gibbs Free Energy =	0.024708
Sum of electronic and zero-point Energies =	-283.268284
Sum of electronic and thermal Energies =	-283.263255
Sum of electronic and thermal Enthalpies =	-283.262311
Sum of electronic and thermal Free Energies =	-283.296725

(Unpolarized solute)-Solvent	(kcal/mol) =	-103.16
(Polarized solute)-Solvent	(kcal/mol) =	-131.19
Solute polarization	(kcal/mol) =	15.64
Total electrostatic	(kcal/mol) =	-115.55

Cavitation energy	(kcal/mol) =	10.19
Dispersion energy	(kcal/mol) =	-14.12
Repulsion energy	(kcal/mol) =	6.89
Total non electrostatic	(kcal/mol) =	2.96
DeltaG (solv)	(kcal/mol) =	-112.60

C,0,0.8466033817,-0.6203034678,-0.0000073777
C,0,-0.4853554425,-0.1435112317,-0.0000144757
O,0,-0.6000718894,1.2733862532,0.0001072424
O,0,-1.5584565743,-0.7962874897,-0.0000505283
N,0,1.9939002317,0.0762785785,-0.0000252531
H,0,1.7543285755,1.0701009599,-0.0000568726
H,0,-1.5561283404,1.401016654,0.0001214538
H,0,0.9201460576,-1.7085792564,0.0000258112



19-3 in Supplementary Fig. 13.

SCF Done: E(UB3LYP) = -283.328321210 Hartree
<S**2>= 0.7547 S= 0.5024

Zero-point correction =	0.052964 (Hartree/Particle)
Thermal correction to Energy =	0.058066
Thermal correction to Enthalpy =	0.059011
Thermal correction to Gibbs Free Energy =	0.024404
Sum of electronic and zero-point Energies =	-283.275357
Sum of electronic and thermal Energies =	-283.270255
Sum of electronic and thermal Enthalpies =	-283.269311
Sum of electronic and thermal Free Energies =	-283.303917

(Unpolarized solute)-Solvent	(kcal/mol) =	-70.90
(Polarized solute)-Solvent	(kcal/mol) =	-83.44
Solute polarization	(kcal/mol) =	7.00
Total electrostatic	(kcal/mol) =	-76.43

Cavitation energy	(kcal/mol) =	10.15
Dispersion energy	(kcal/mol) =	-13.70
Repulsion energy	(kcal/mol) =	4.11
Total non electrostatic	(kcal/mol) =	0.55
DeltaG (solv)	(kcal/mol) =	-75.88

C,0,0.6535101562,-0.7269551074,-0.0822028045
 C,0,-0.6178524639,0.0386750088,0.0184378894
 O,0,-0.4799448675,1.3032981995,0.0330885988
 O,0,-1.6833701433,-0.632359496,0.0910624685
 N,0,1.8399077817,-0.0159352668,-0.2762782721
 H,0,2.6523283712,-0.3428413035,0.2356028659
 H,0,1.6305662679,0.9712935049,-0.1171995321
 H,0,0.6864618977,-1.8103645395,-0.1012862139

1.8. *In vitro* Susceptibility Testing

Bioassays of NOS and 5'-fluoro-NOS (27) against *B. subtilis*. 0.1 µg, 0.2 µg, 0.4 µg or 0.8 µg of each compound in 100 µl of THF was added to stainless steel cylinders on Antibiotic Medium 2 (purchased from SCAS EcoScience Technology Inc., China) agar plates that were pre-seeded with an overnight culture of the test strain at a concentration of 1% (vol/vol). The plates were incubated at 37°C for 20-24 hrs, and the biological activity was estimated by measuring the sizes of the inhibition zones. All assays were carried out in triplicate.

Minimum Inhibitory Concentrations (MICs) of NOS and 5'-fluoro-NOS (27). The MICs were measured by broth dilution similar to the method described previously¹⁵. Each test compound was dissolved in THF to produce a stock solution (10 µg/ml), which was serially diluted into 50 µl Mueller-Hinton broth (Qingdao Hope Bio-Technology Co. Ltd., China) in a 96-well microtiter plate to a final concentration ranging from 0.0256 to 0 µg/ml. 50 µl of the test strain (10^7 - 10^8 cfu/ml, calculated according to the 0.5 McFarland standard¹⁶) was then added into each well of the microtiter plate. After incubation at 37°C for 18-24 hr, The MIC was determined to be the lowest concentration of compound that inhibited visible bacterial growth. All testings were carried out in duplicate.

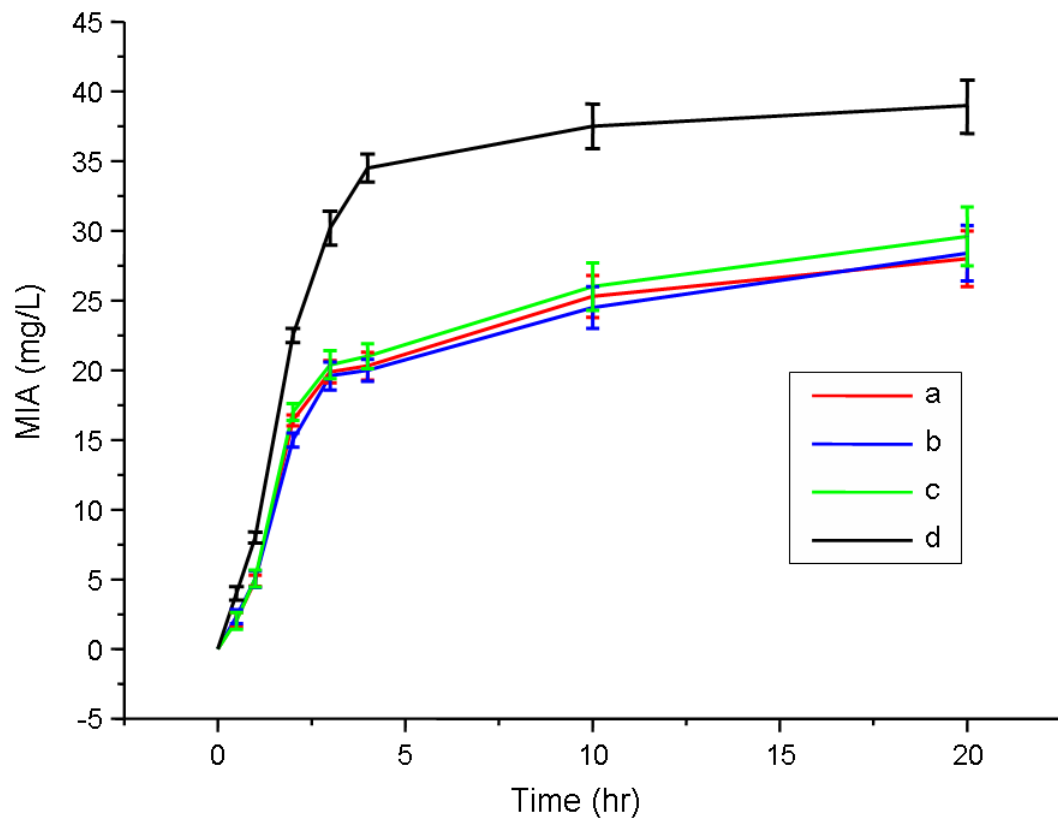
2. Supplemental Results

2.1 Supplementary Figures

Supplementary Figure 1. Time course analysis of MIA production in the *nosL*-expressing strain SL4101.

Without the supplementation (a, control), and with the supplementation of Gly (b), L-Ser (c), and L-Trp (d),

respectively. Data represent mean values \pm s.d.



Supplementary Figure 2. Multiple sequence alignment of selected radical S-AdoMet proteins, including NosL from *S. actuosus* (ACR48341), ThiHs from *Salmonella enterica* (AAD48429) and *E. coli* (AAB95619), BioB from *E. coli* (CAQ31276), PflA from *E. coli* (CAQ31430) and KamA from *Thermoanaerobacter tengcongensis* (AAM23985). For site-specific mutations, the conserved motif CxxxCxxC for [4Fe-4S] nucleating and the G residue in the S-AdoMet binding site are boxed. NosL shares around 20% sequence identity to various ThiHs, but no significant homology to others in overall sequence.

```

NosL_S.actuosus  --MTQNSQAMTSHAMTGDVFLPELEDVRAEAATVDTRAVLALAEGEPAESRAAVLALME
ThiB_S.enterica -----MRTFTDRWROLEWDDIRLR--INGRTAADVERALNAABLSRDDIMALLS
ThiB_E.coli      -----MRTFSDRWROLDWDDIRLR--INGRTAADVERALNASQITRDDMMALLS
BioB_E.coli      -----MARRPRWTLISQVTELFERPLLDLILFEAQ
PflA_E.coli      -----MSVIGRITRS
KamA_T.tengcong MRVVRREBELFGHVPSDINYNWRWQIANRIETVEELRKYLP LSEEEEAISKALQQLRMAI
consensus      -----t--w-q-ewedvr-----y-k---l-g-e-a----dllal-#

NosL_S.actuosus  DRSIGTAELOQAAREARCGARRP--RIHTFVP-----L
ThiB_S.enterica  PAAADYLEPIAQRARLTRQRFGNTVSPFYVE-----L
ThiB_E.coli      PAASGYLEQLAQRARLTRQRFGNTVSPFYVE-----L
BioB_E.coli      QVHRQHFDPQVQVSTLLS-----F
PflA_E.coli      FESCSTVDGPGIR-----FIT-----F
KamA_T.tengcong TPYYLSLIDPMDPNDPIRRRAVPTIBELYQAPEDLVDPDYEDVDSFPVPGLTRYPDRVLM
consensus      -----gtle--a-r--rl-r-r---l--yvp-----l

NosL_S.actuosus  YTMNYCDSECRKCSMRRGMRRLDRKFSGRKEITEQLEILYHBEGVRGVGLLIGEYEDKRT
ThiB_S.enterica  YLSMIGANDCTYCGFSMSM-RIRRRTLDEVDIQRECDAIR-RLGPEHLLLVIGEBQARVG
ThiB_E.coli      YLSMIGANDCTYCGFSMSM-RIRRRTLDEVDIQRECDAIR-EMGPEHLLLVIGEBQARVG
BioB_E.coli      IRTGACPEDCRYCQGS-SRYKTLGAERIMEVEQVLESARKARAAAGSTRFCGAAWKNPE
PflA_E.coli      FQG--CLMRCLYCHNRDITWDTGGGKVTVEILMKREVVTYR-----HFMNASGGVVTASG
KamA_T.tengcong  LWEDCCSMYCRBCERRRFAGETDAP-MPMDRIEKQIEYIKNTPOQRDVLISGAPLTLSD
consensus      yltr-C--dCkyC-----sn-rl-rk-l-l-di-rele-ir--g--hvlllltGf--k-g

NosL_S.actuosus  RLASAFRIGWAIRTAIDLGFERYVFNIGSMEQDEIDVLGEMIGREDPVVTCVQESYDRE
ThiB_S.enterica  --MDYFRR--HLPTLRQFSSLOMEVQPLSQENYAEI-KTLGIDG---VMVYQETVHEA
ThiB_E.coli      --MDYFRR--HLPALREQFSSLOMEVQPLAETIYAEI-KQLGIDG---VMVYQETVHEA
BioB_E.coli      -----ERDMPYLEQMVQGVKAMGLEACMTLGTLSSESQAQRLANAG-----LDYINEN
PflA_E.coli      -----GEAIIQAEFFVRDMPFRACKREG-----ITCILDITNG-----FVRYDVPV
KamA_T.tengcong  S-----RLEEIIRRLREIPEVEIIRIGSSVPPVVLPMRITPELVN-----MLKRYHPPI
consensus      -----frr---l--lr--f--v-mei-m--t---l---lg-eg---m-vfqe#Yh--

NosL_S.actuosus  TYRRFMGRTSVGVPRADFDRRVVVSPDRWLDAGYRYVNPGLVVG-LHDDLSAEIIVSLVAEG
ThiB_S.enterica  TYAQHHILRG---RRQDFPWRLETPDRLGRAGIDKIGLGALIG-LSDNMRVDCYVVAEHL
ThiB_E.coli      TYARHHILRG---RRQDFPWRLETPDRLGRAGIDKIGLGALIG-LSDNMRVDCYVVAEHL
BioB_E.coli      LDTSPEFYG-NIITTRTYQERLDTELRVVDAGIRVCSGGIVG--LGETVDRAGILLQLA
PflA_E.coli      IDELLEVTD-----LVMILDLKQ-MNDEIIBQNLVGVSWER
KamA_T.tengcong  WLNTHFNHP-----HEITEDSKRACEMLDADAGIPLGNQTVLLRGVMDCVVVMKRIIVREIL
consensus      iy--h-lkg-----k-df--rlet-drlgdagi--v-lgvlvg-l-d-lrve--mv-ehl

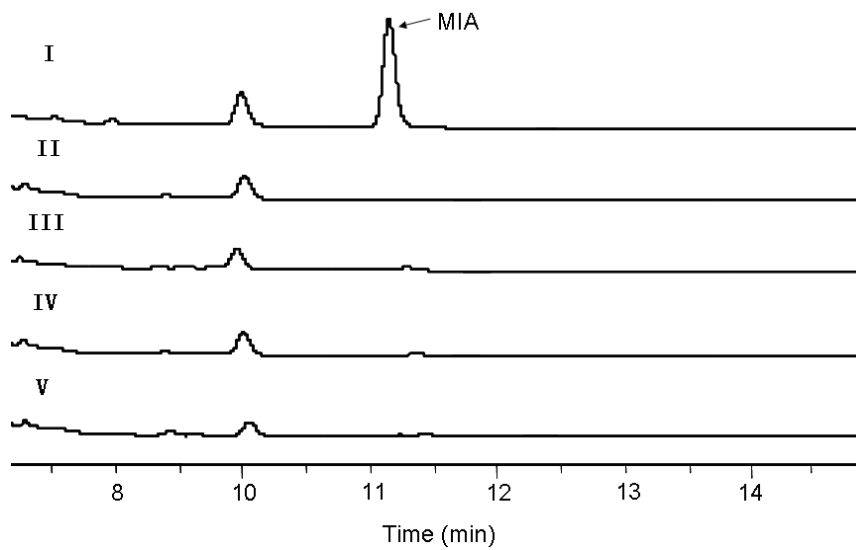
NosL_S.actuosus  DILRSR--GATADLSVPRMRFAMRSRDTTRVGD-DYTLRLMSVVAFTCPAQRIIVLTREP
ThiB_S.enterica  LWMQKHYSQSRYSVSPFRIIRPCTGGVEPASVMDERQLVQTCIFAPRLLAPETIELSLSTRES
ThiB_E.coli      LWMQKHYSQSRYSVSPFRIIRPCTGGVEPASVMDERQLVQTCIFAPRLLAPETIELSLSTRES
BioB_E.coli      NLTPTPPESVPLNMLVXVGTPLADMD---VDAPDFIRTIAVARIMMPTSYVRLSAGRE
PflA_E.coli      TLEFARYLANRNVVWIRYVVVPG-----WSDDDSAERLGEFTRDMGNVRIEILLYPH
KamA_T.tengcong  RIRVRPYYIYQCDLSEFGLSEFRTPVSRGIEILEG--LRGTSYGYCVPTFVVVDFAPGGGRI
consensus      -ll--yw--r--l-fprprp-tg--d---vadd-dll-ti-afill-peiel-lstre-

NosL_S.actuosus  QEFQDVALGLAGVISPGSPDVAPYRAGCEARNDEKSSQFLVADLRKPRHILGRIEASGTP
ThiB_S.enterica  PWFPRDVIPLA---INNVSAFSEKTPGGYADHPELEQFSPEDARRPETVASALSQAQGLQ
ThiB_E.coli      PWFPRDVIPLA---INNVSAFSEKTPGGYADHPELEQFSPEDARRPEVAVAALTAQGLQ
BioB_E.coli      QMNEQTQAMCPMAGANSIPYGCRLITTPNPEEDKDLQLFRKLLGLNPPQQTAVLAGDNEQQQ
PflA_E.coli      ELGRKRWVANG-----BEYKLDGVRPFRKREMERVGRGILBQYGRK
KamA_T.tengcong  PVGPNYVISQSHDRIVLRMYEGVIVTYVEPRRITPDPGVCVDEEVPKSEGVAGILMQDITG
consensus      pafrd-vi-la---in-v---k---g--add-eleqf-p-dlrrpe-vagalea-glq

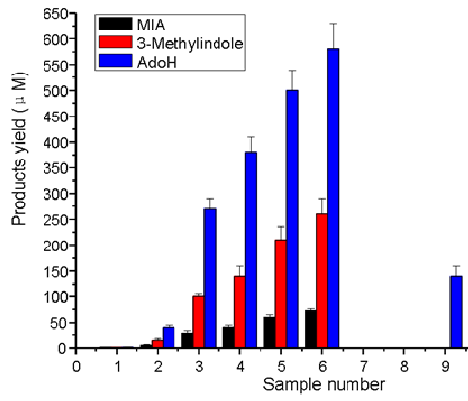
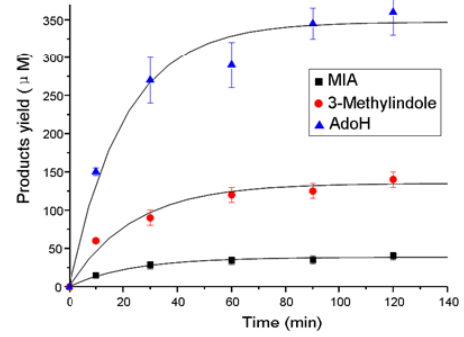
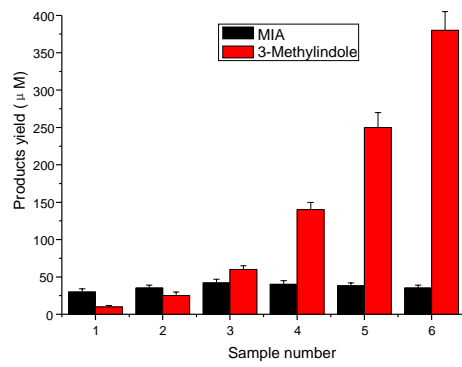
NosL_S.actuosus  --VDBFVNPAGEASRAV--
ThiB_S.enterica  PVWRDWDSSLGRASQTR---
ThiB_E.coli      PVWRDWDSSLGRASQRL---
BioB_E.coli      RLQALMTPDTEYYNAAL
PflA_E.coli      VMF
KamA_T.tengcong  VLEPEMLERKRRRRRDER--
consensus      -v-dfvs--gras-----

```

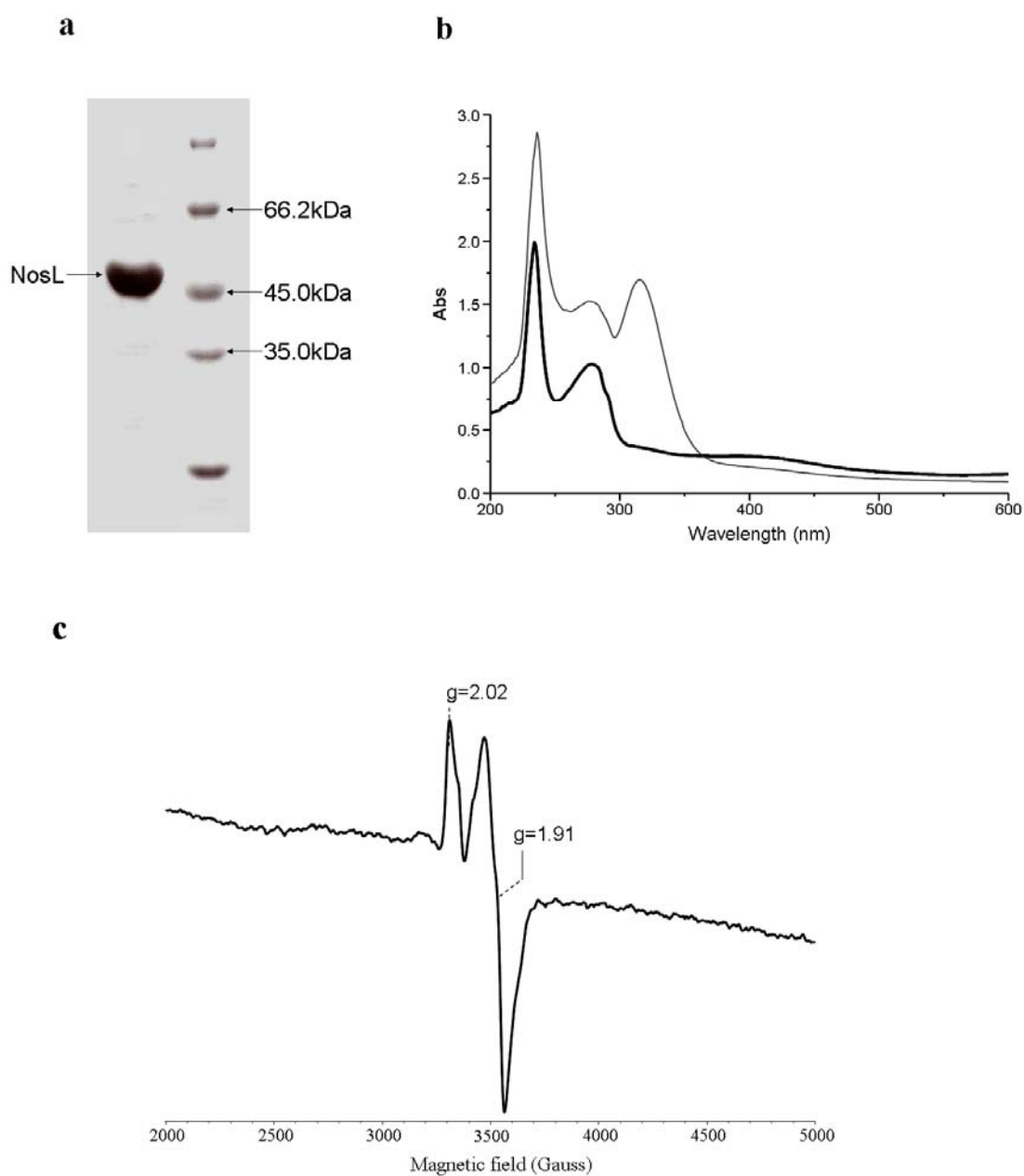
Supplementary Figure 3. HPLC analysis of MIA production in the recombinant *E. coli* strains. SL4101 for expressing NosL (I), SL4103 for expressing the C95A mutant NosL (II), SL4105 for expressing the C99A mutant NosL (III), SL4107 for expressing the C102A mutant NosL (IV), and SL4109 for expressing the G142A mutant NosL (V).



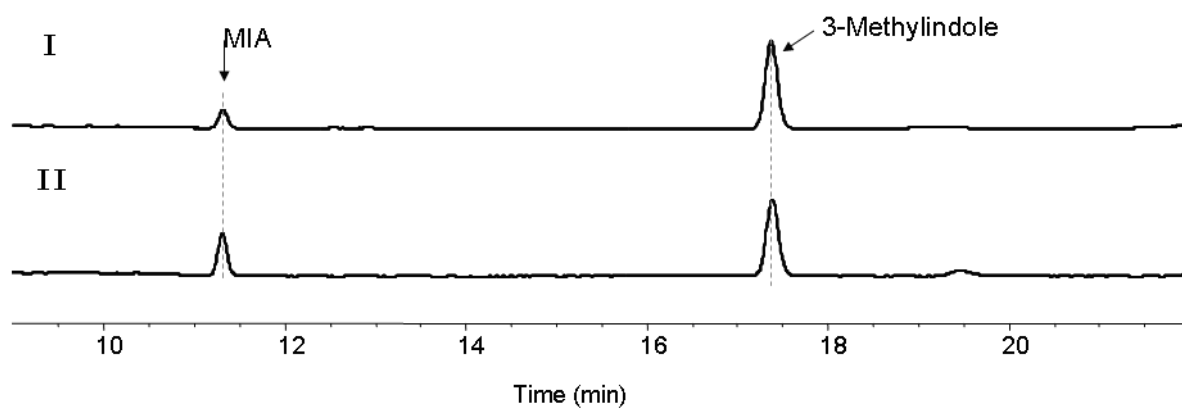
Supplementary Figure 4. Quantitative analysis of NosL-catalyzed *in vitro* conversion. (a) Dependence of enzyme concentration. The reactions are catalyzed by 20 μM aerobically purified NosL (Sample 1), 20 μM anaerobically purified NosL (without reconstitution, Sample 2), and 10 μM (Sample 3), 20 μM (Sample 4), 40 μM (Sample 5), or 80 μM reconstituted NosL (Sample 6), respectively, in the presence of *S*-AdoMet, L-trp and dithionite. Samples 7, 8 and 9 served as the controls, by respectively omitting NosL, *S*-AdoMet, and L-trp from Sample 4. (b) Time course of NosL-catalyzed *in vitro* conversion for detecting the production of MIA, 3-methylindole, and AdoH. The reaction mixture contains reconstituted NosL (20 μM), L-trp (500 μM), *S*-AdoMet (1 mM) and sodium dithionite (1 mM). (c) Effect of dithionite concentration on the production of MIA and 3-methylindole. Each 100 μM of reaction mixture, containing 20 μM reconstituted NosL, 10 mM dithiothreitol, 1 mM *S*-AdoMet, 500 μM L-Trp, and dithionite varying in concentration in 50 mM Tris-HCl buffer (pH 8.0), was carried out at 25°C for 2 hr before product examination. Samples 1-6 show the concentration of dithionite at 100 μM (1), 200 μM (2), 500 μM (3), 1 mM (4), 2 mM (5), and 4 mM (6), respectively. Data represent mean values \pm s.d.

a**b****c**

Supplementary Figure 5. Characterization of the reconstituted NosL. (a) NosL (48.4 kDa) on the 12% SDS-PAGE gel. (b) UV-Vis absorptions of the reconstituted protein (bold line) and the protein reduced by sodium dithionite (thin line). (c) EPR spectrum of reconstituted NosL reduced by sodium dithionite. The values were recorded under the following conditions: temperature, 13 K; modulation amplitude, 5 G; microwave power, 1.0 mW; and microwave frequency, 9.4 GHz.



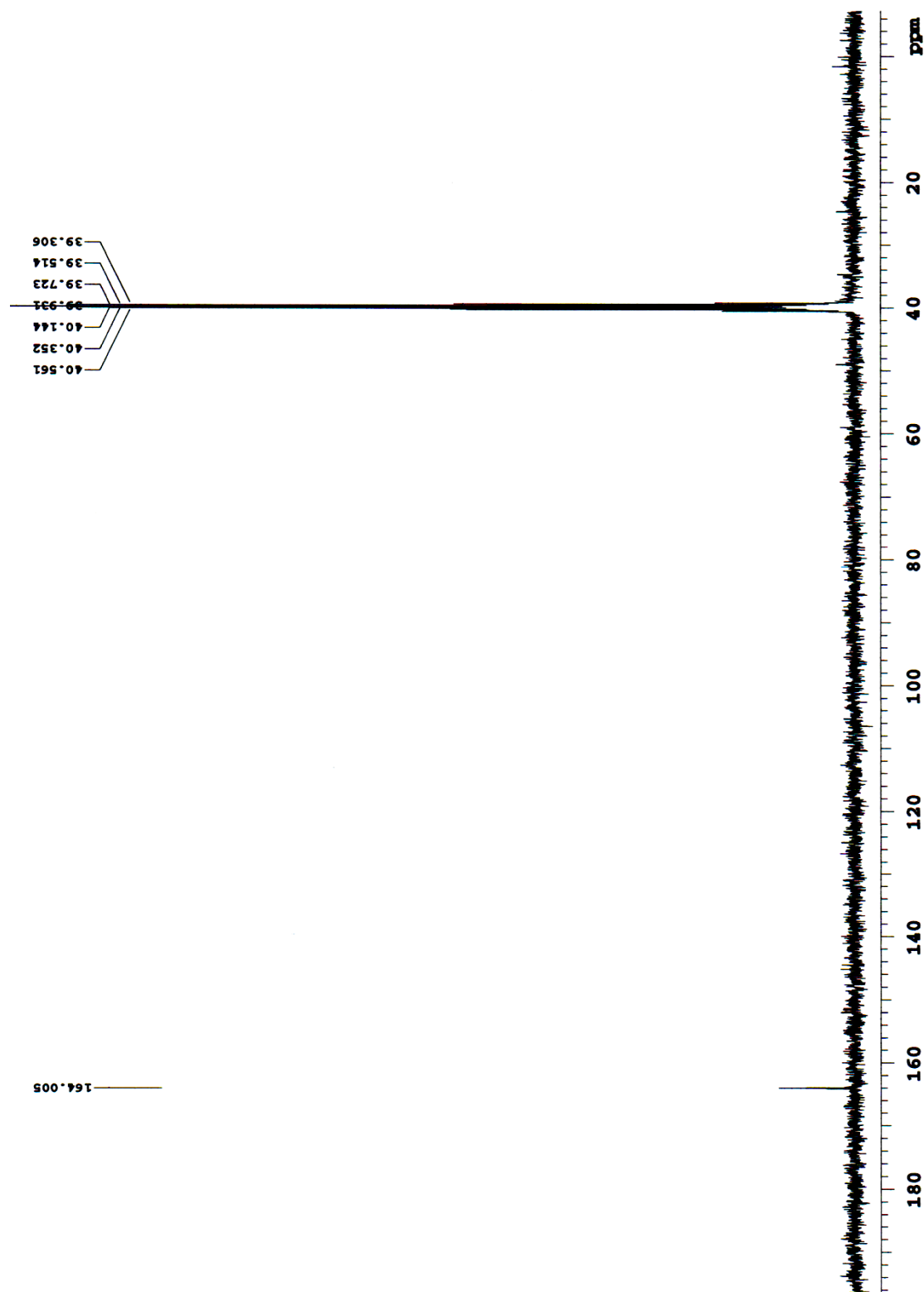
Supplementary Figure 6. NosL-catalyzed MIA production *in vitro*. I, in the presence of the chemical reductant dithionite; and II, in the presence of the natural reduction system (flavodoxin, flavodoxin reductase, and NADPH).



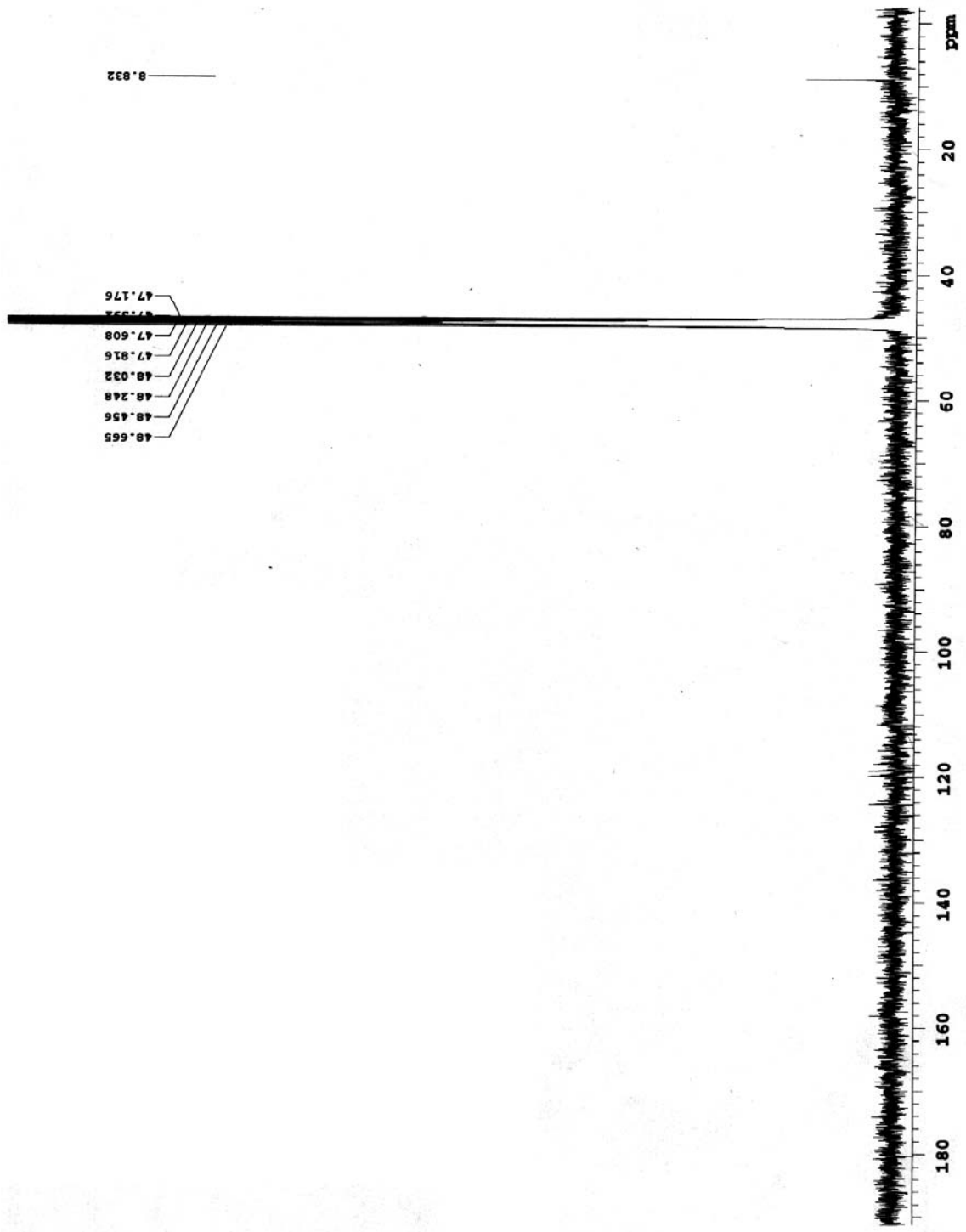
Supplementary Figure 7. ^{13}C NMR spectra (100MHz, $\text{d}_6\text{-DMSO}$) of labeled MIAs. (a)

[carboxyl- ^{13}C]MIA (3), (b). [methyl- ^{13}C]MIA (4).

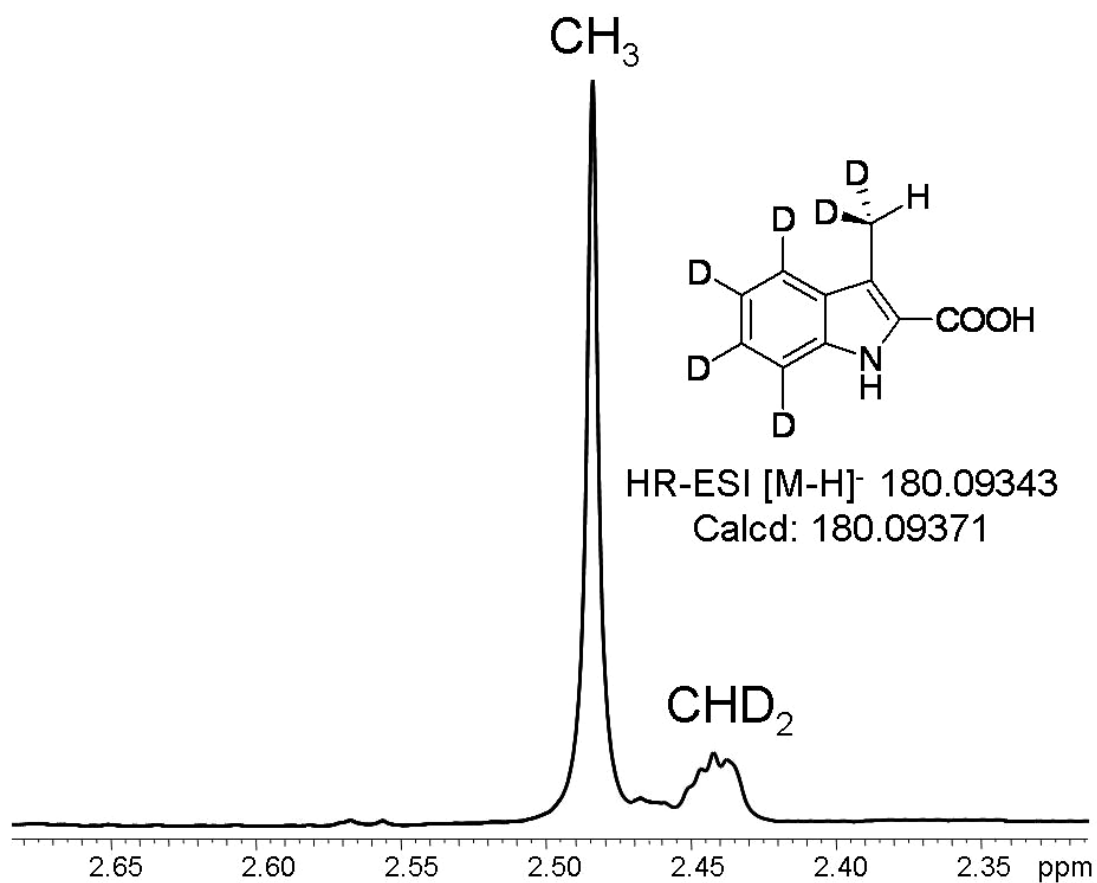
a



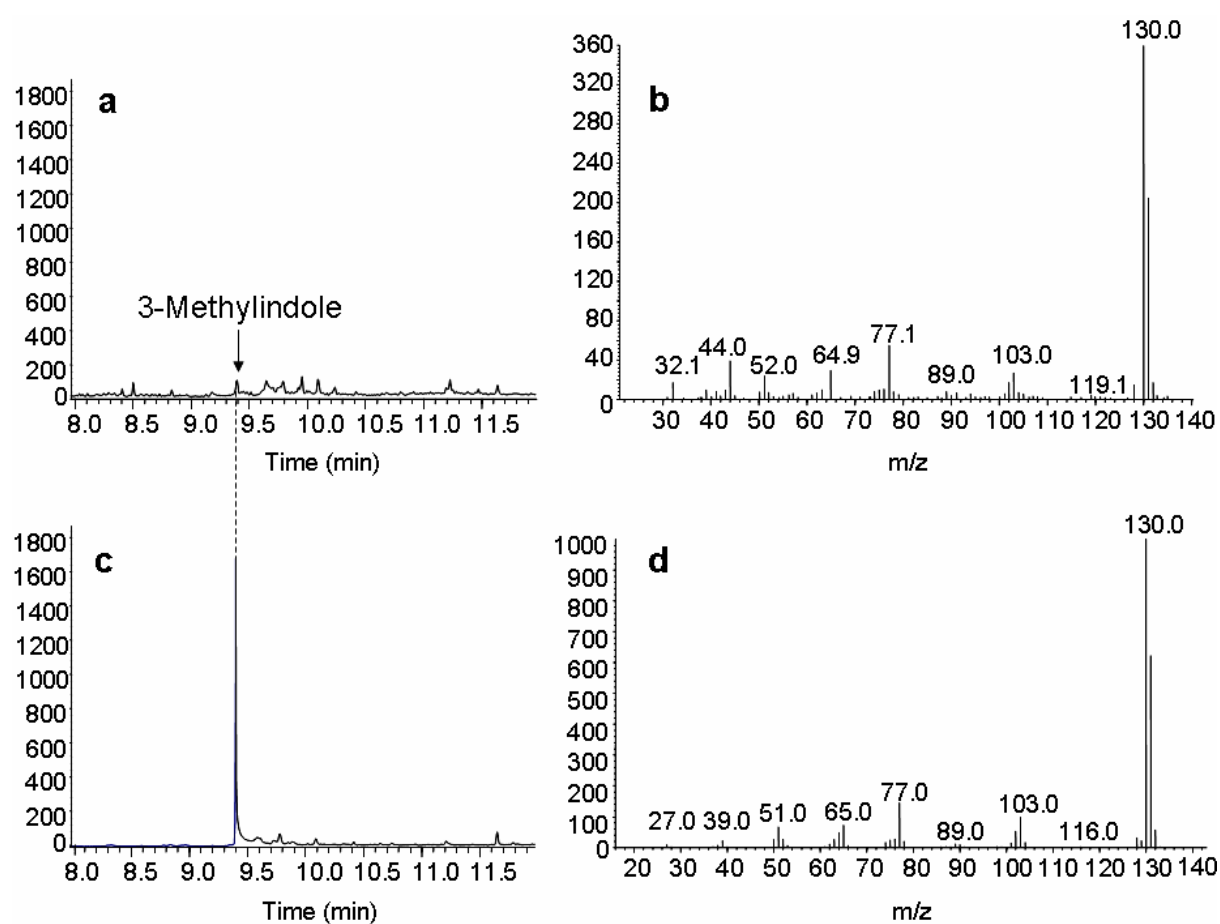
b



Supplementary Figure 8. Partial ^1H NMR spectrum (500MHz, CD_3OD) of the mixture of MIA (1) and $[\text{}^2\text{H}_6]\text{MIA}$ (5), produced by feeding L- $[\text{}^2\text{H}_8]\text{Trp}$ into the *NosL*-expressing *E. coli* strain SL4101.

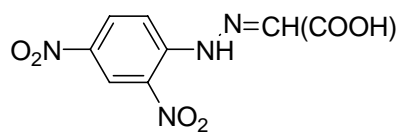


Supplementary Figure 9. GC-EI-MS analysis of 3-methylindole (**6**) production in NosL-catalyzed *in vitro* conversion (a and b, respectively, for GC and its coupled EI-MS spectra), using the authentic compound as the standard (c and d, respectively, for GC and its coupled EI-MS spectra).



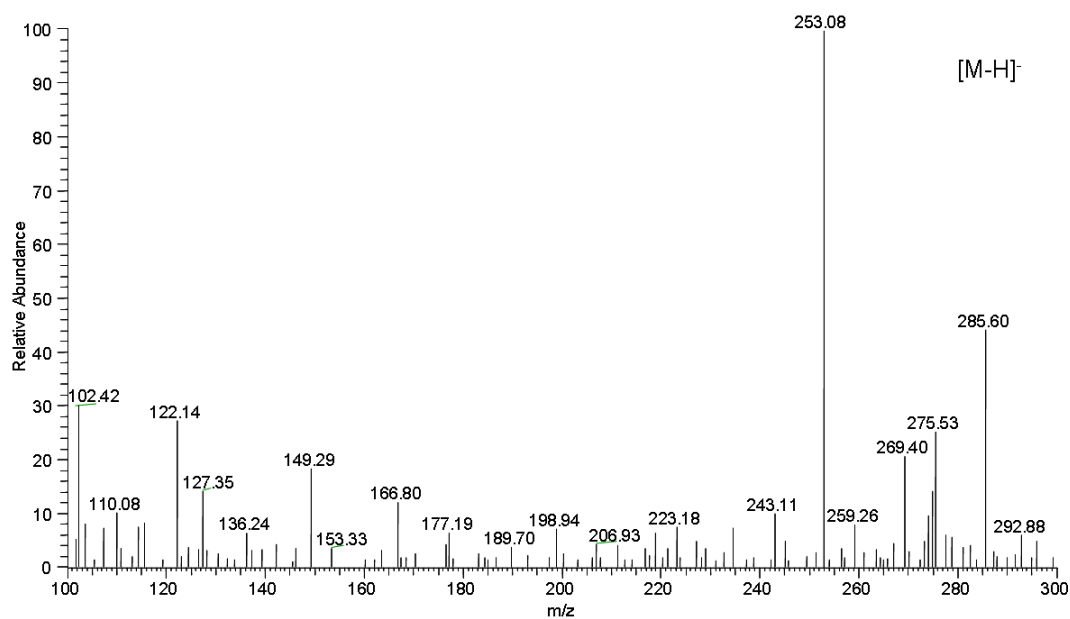
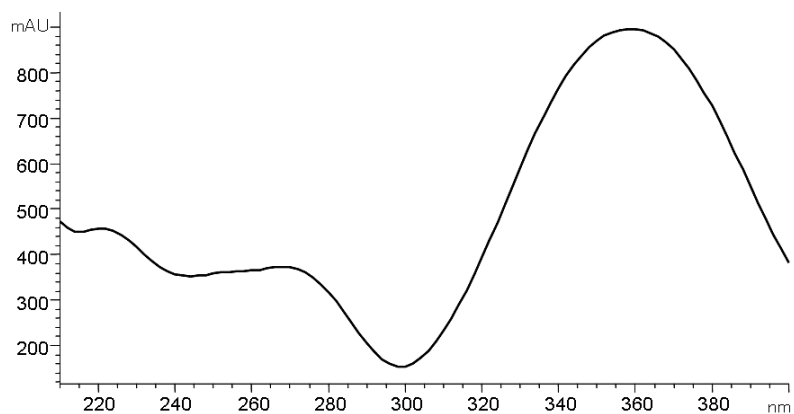
Supplementary Figure 10. Characterization of glyoxylate-NDP (**8**), the derivative of glyoxylate (**7**) in

NosL-catalyzed *in vitro* conversion, showing the structure, UV absorption, and negative mass ionization.



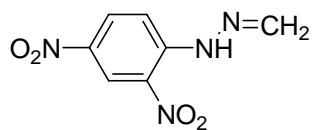
Chemical Formula: $C_8H_6N_4O_6$

Molecular Weight: 254.03



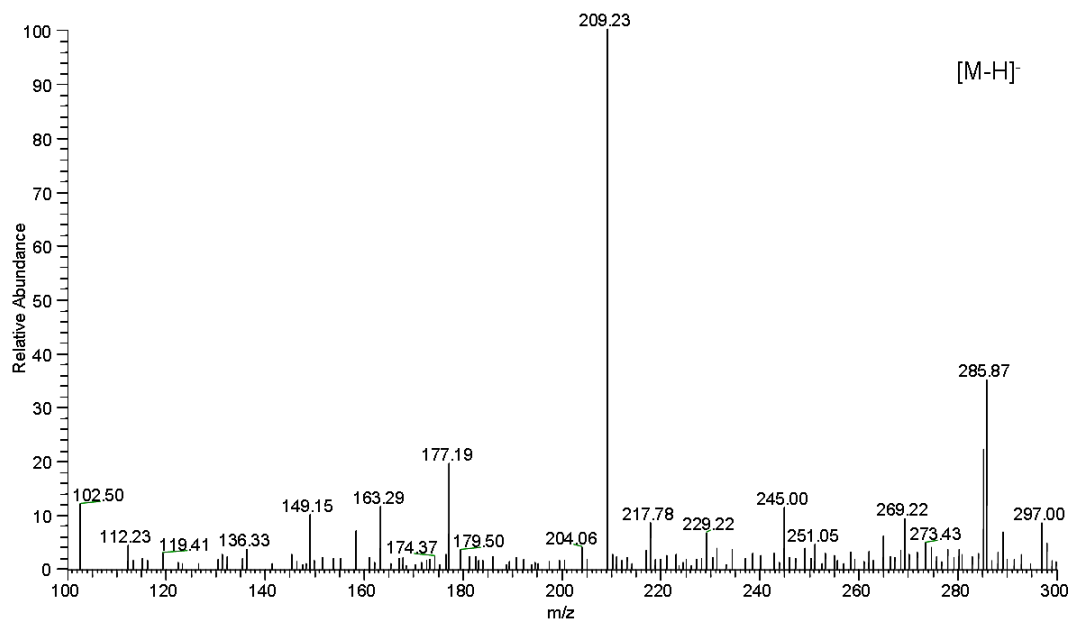
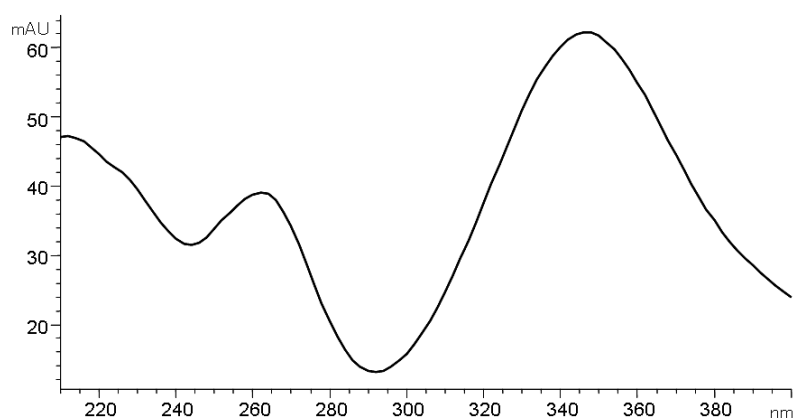
Supplementary Figure 11. Characterization of formaldehyde-NDP (**10**), the derivative of formaldehyde (**9**)

in NosL-catalyzed *in vitro* conversion, showing the structure, UV absorption, and negative mass ionization.

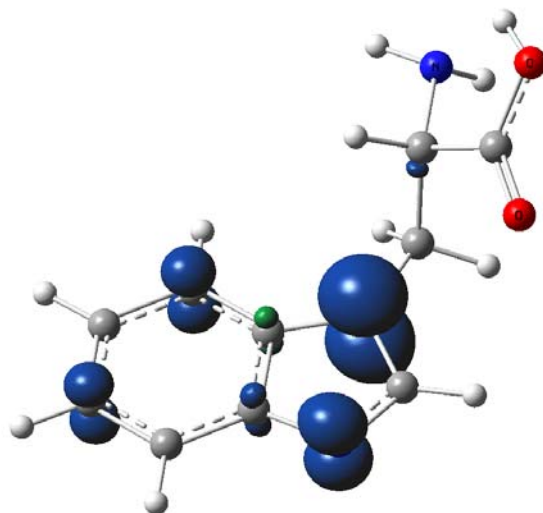


Chemical Formula: C₇H₆N₄O₄

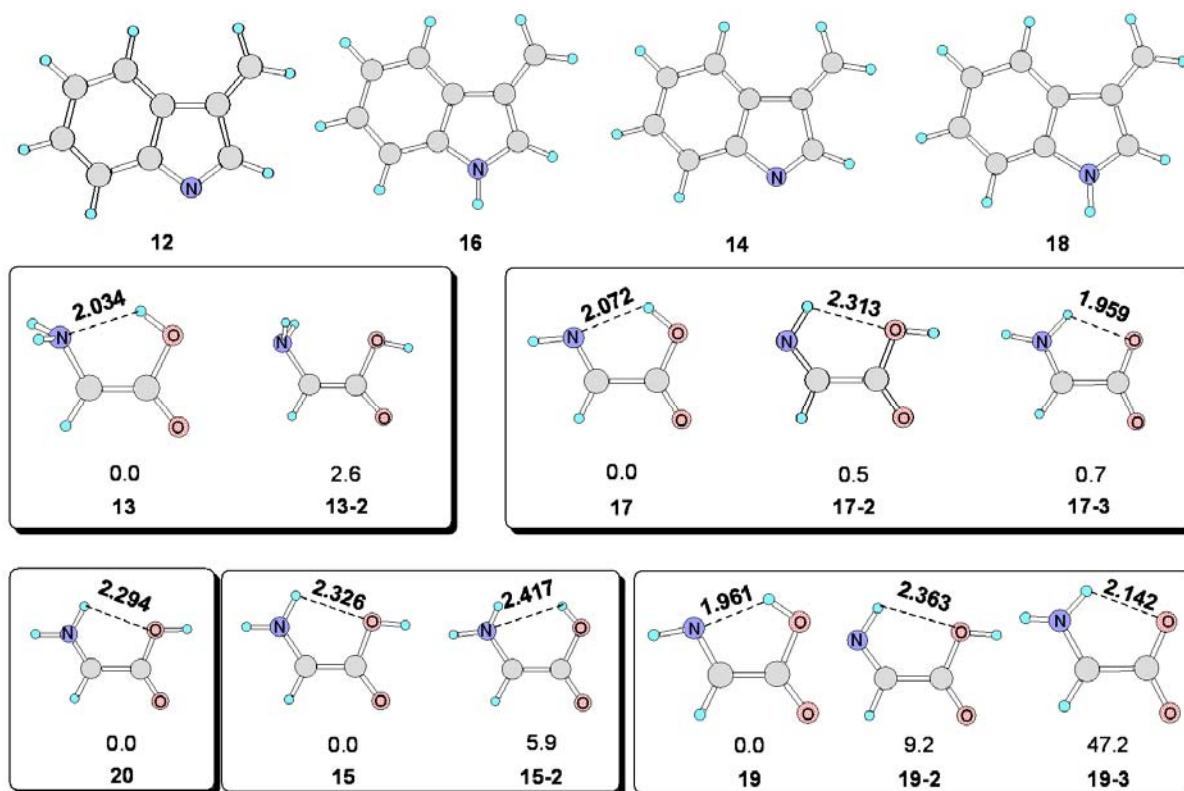
Molecular Weight: 210.04



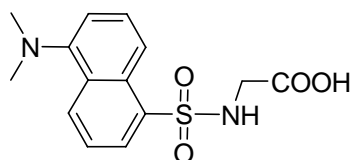
Supplementary Figure 12. Plot of the spin densities of L-Trp neutral radical (**11**). Most of the spin densities of **11** are distributed on the indole C3.



Supplementary Figure 13. Structures and relative free energies of the cleavage products of L-Trp neutral radical (11). 13-2 is the possible isomer of 13, 17-2 and 17-3 are the possible isomers of 17, etc. The relative free energies including solvent effect ΔG_{sol} are in kcal/mol.

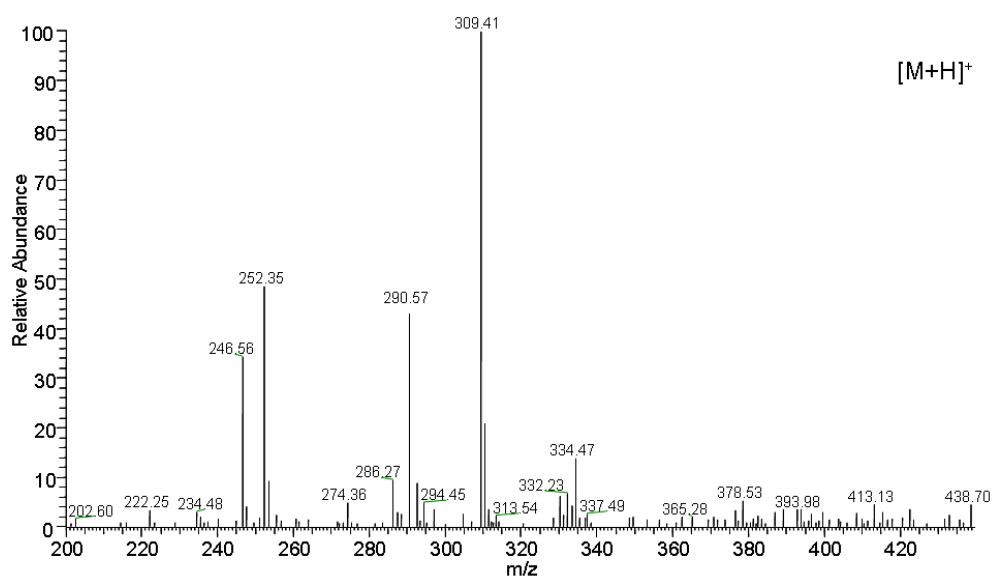
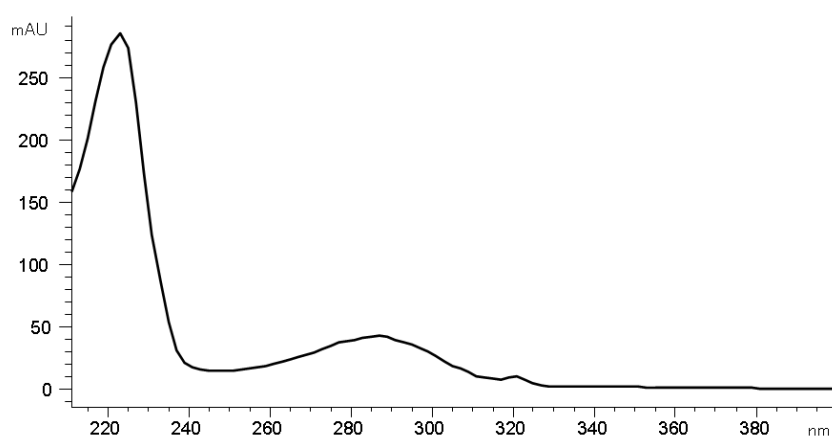


Supplementary Figure 14. Characterization of Gly-Dansyl (**22**), the putative derivative of glycine radical (**21**) in NosL-catalyzed *in vitro* conversion, showing the structure, UV absorption, and positive mass ionization.

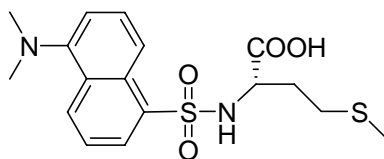


Chemical Formula: $C_{14}H_{16}N_2O_4S$

Molecular Weight: 308.03

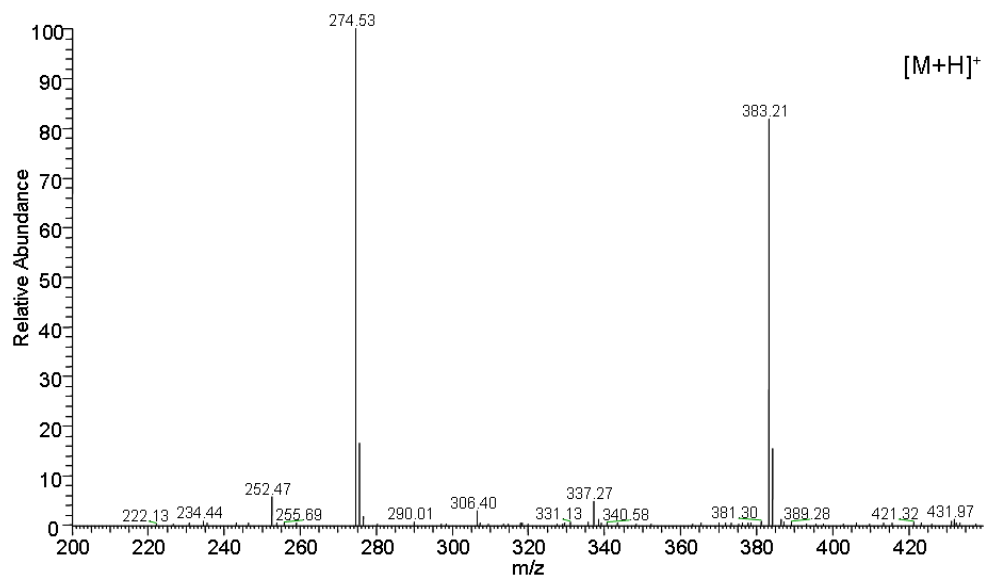
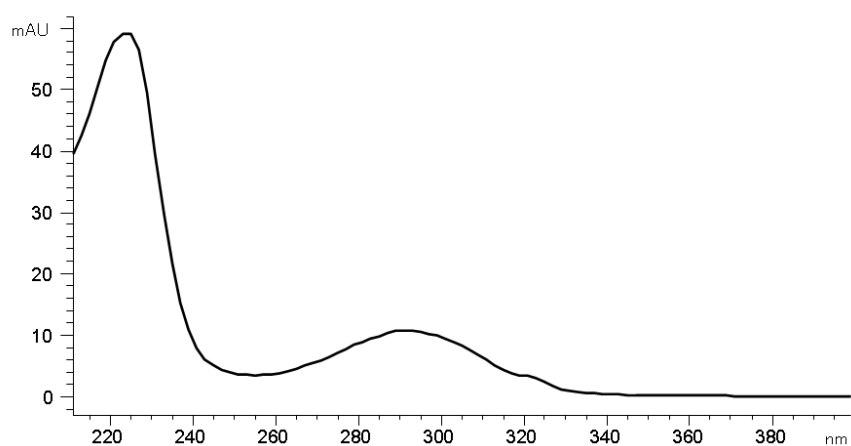


Supplementary Figure 15. Characterization of Met-Dansyl (**24**), the derivative of L-Met (**23**) in NosL-catalyzed *in vitro* conversion, showing the structure, UV absorption, and positive mass ionization.

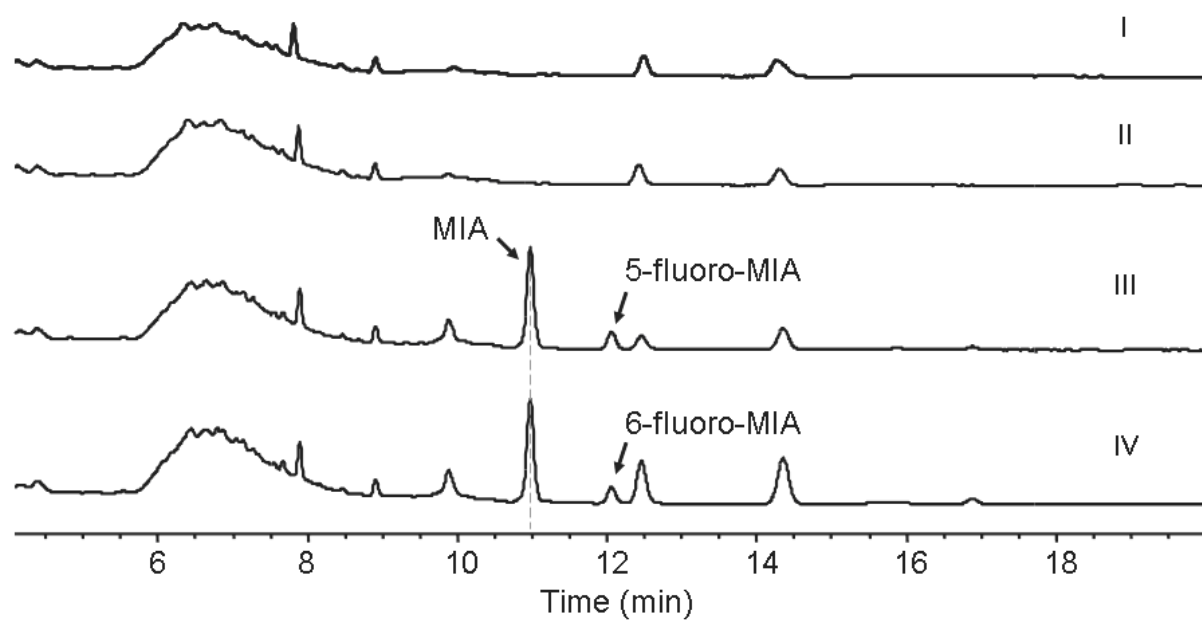


Chemical Formula: $C_{17}H_{22}N_2O_4S_2$

Molecular Weight: 382.10



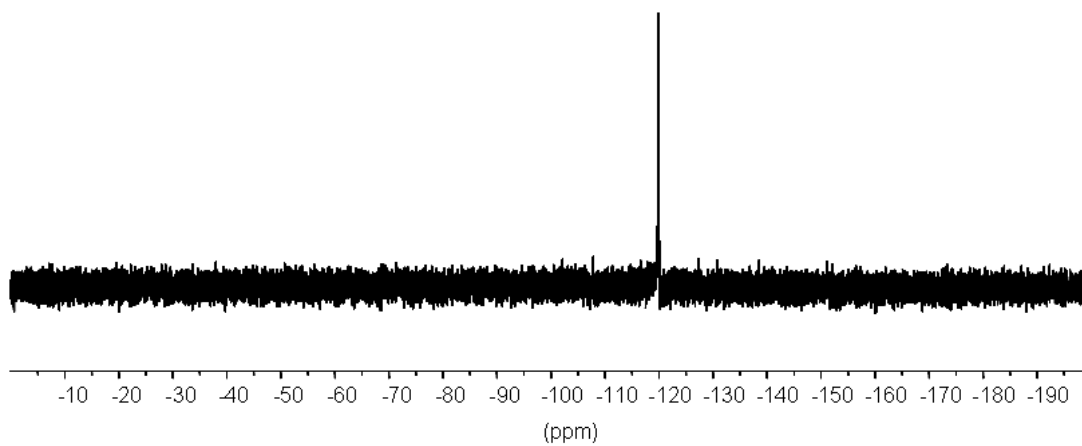
Supplementary Figure 16. HPLC analysis of the production of fluorinated MIAs in *E. coli* strains. SL4100 (carrying the vector pET28a) with the supplementation of 5-fluoro-DL-Trp (I) and 6-fluoro-DL-Trp (II), respectively, and SL4101 (*nosL* expressing) with the supplementation of 5-fluoro-DL-Trp (III) and 6-fluoro-DL-Trp (IV), respectively.



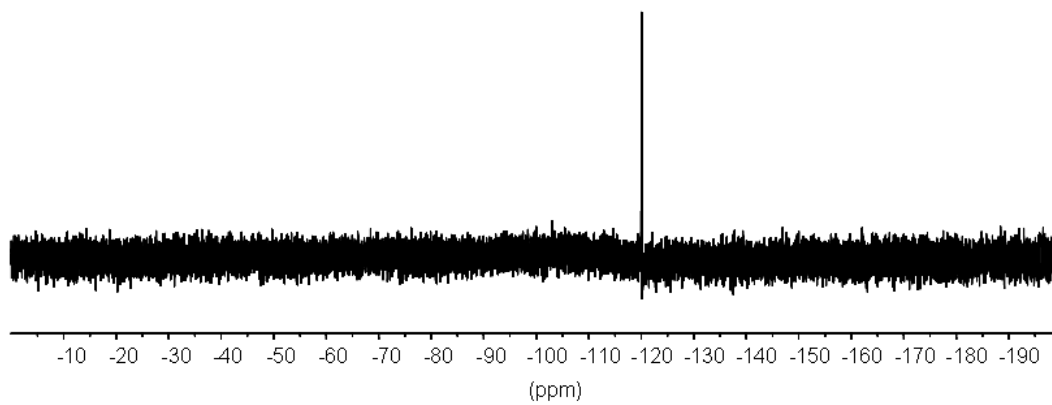
Supplementary Figure 17. ^{19}F NMR spectra of fluorinated MIAs. (a) 5-Fluoro-MIA (**25**). (b)

6-Fluoro-MIA (**26**).

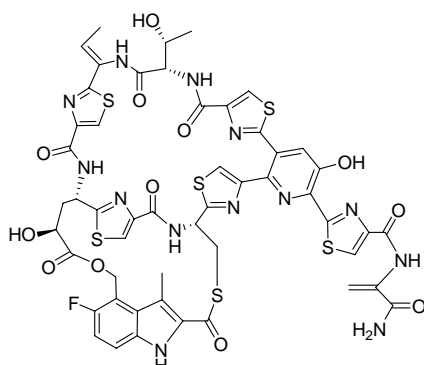
a



b



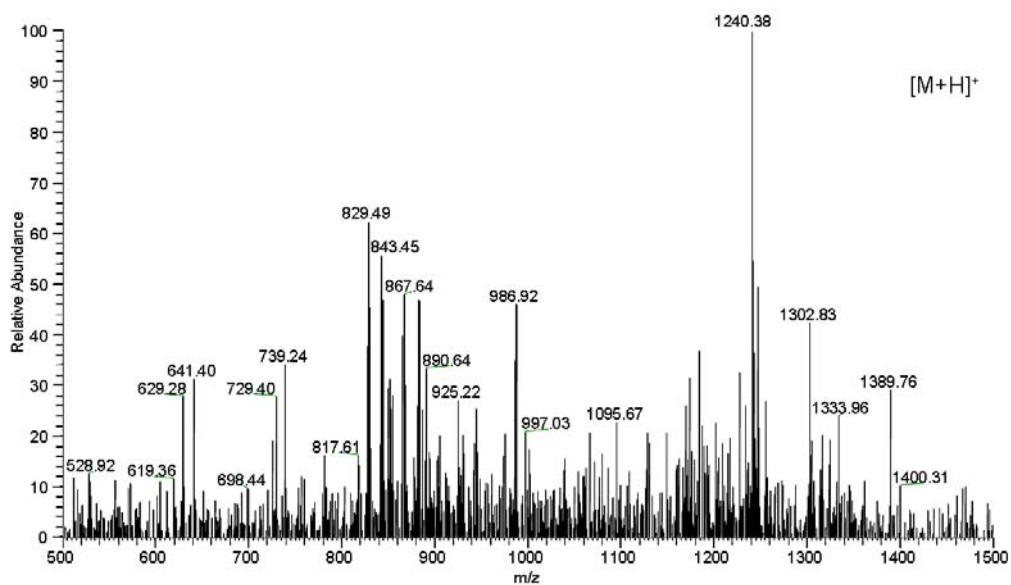
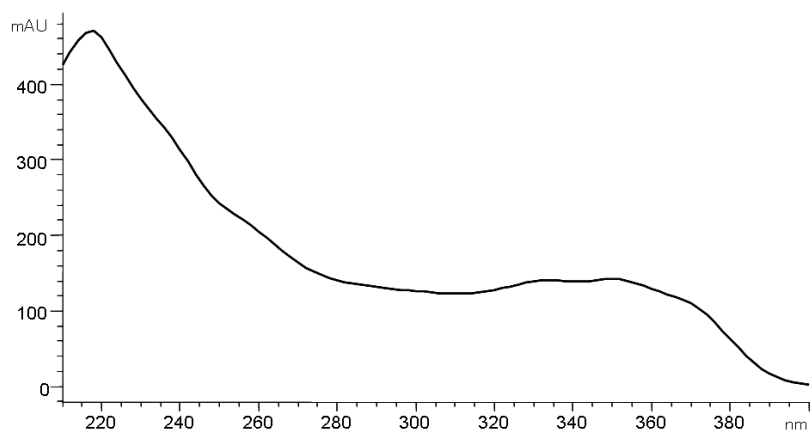
Supplementary Figure 18. Characterization of 5'-Fluoro-NOS (**27**), showing the structure, UV absorptions, and positive mass ionization.



5'-fluoro-NOS, **27**

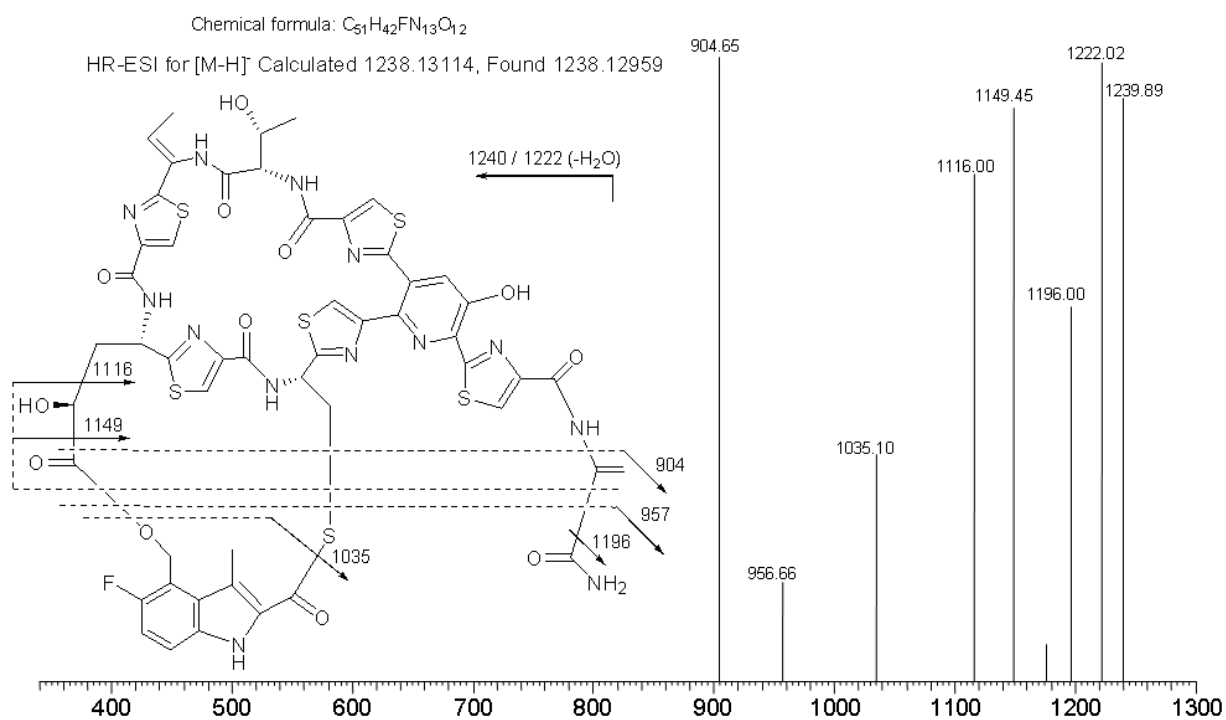
Chemical Formula: $C_{51}H_{42}FN_{13}O_{12}S_6$

Molecular Weight: 1239.14

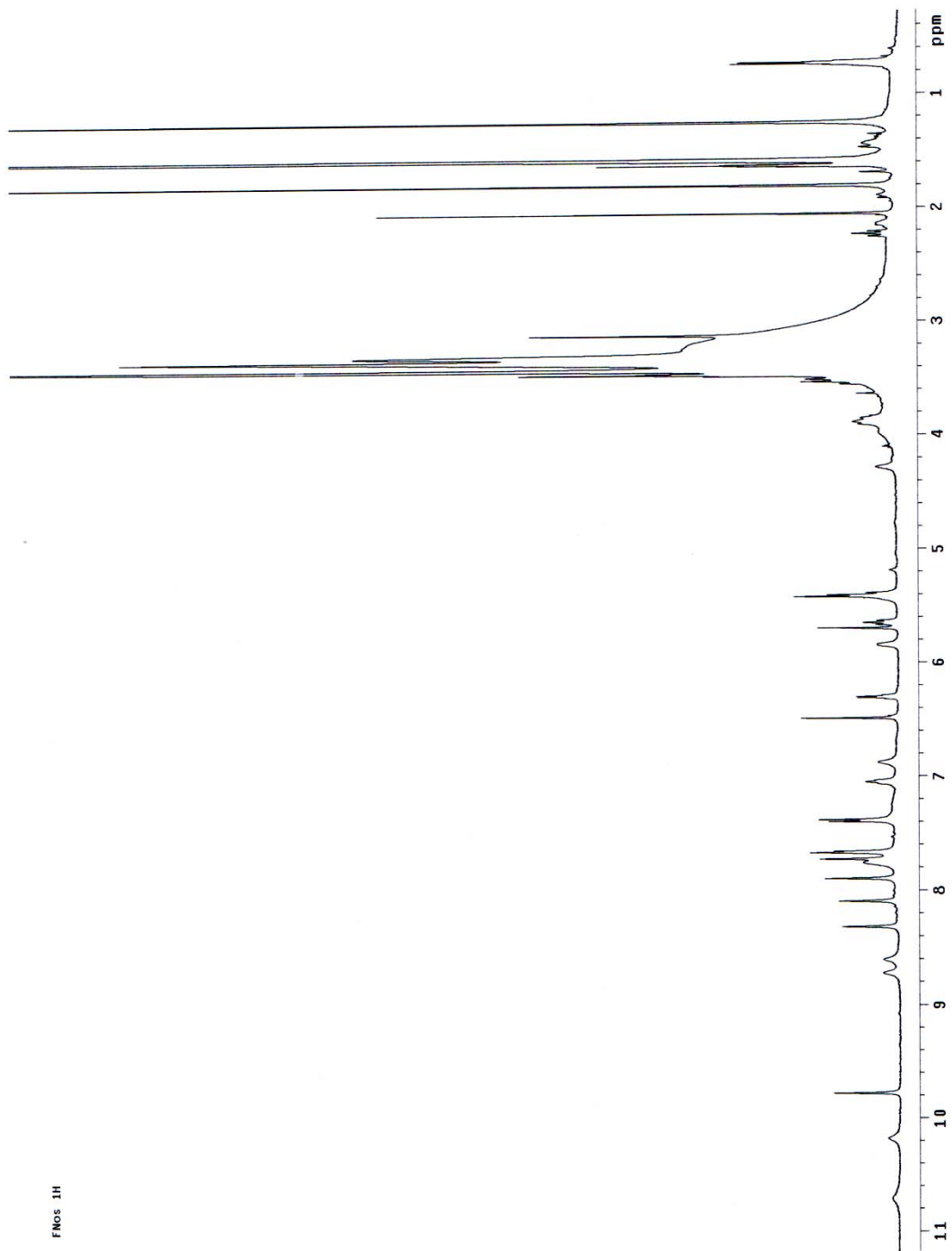


Supplementary Figure 19. Spectra of 5'-fluoro-NOS (**27**) for structural elucidation. (a) ESI-MS/MS spectrum (positive ion scanning). (b) ^1H NMR (600MHz, d_8 -THF). (c) ^{13}C NMR (150MHz, d_8 -THF). (d) ^1H - ^1H COSY (600MHz, d_8 -THF). (e) HSQC (600MHz, d_8 -THF). (f) ^{19}F NMR (376MHz, d_6 -DMSO).

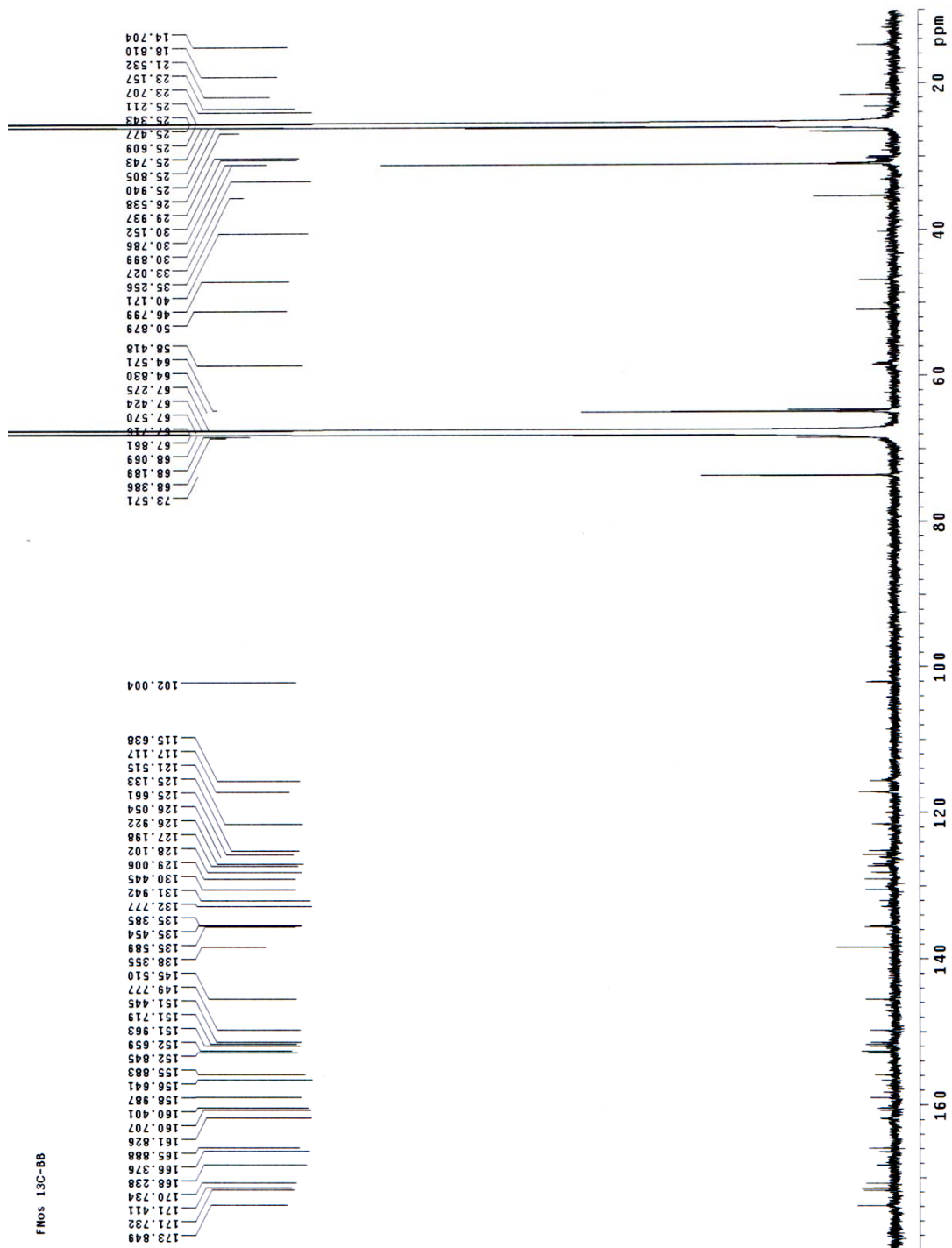
a



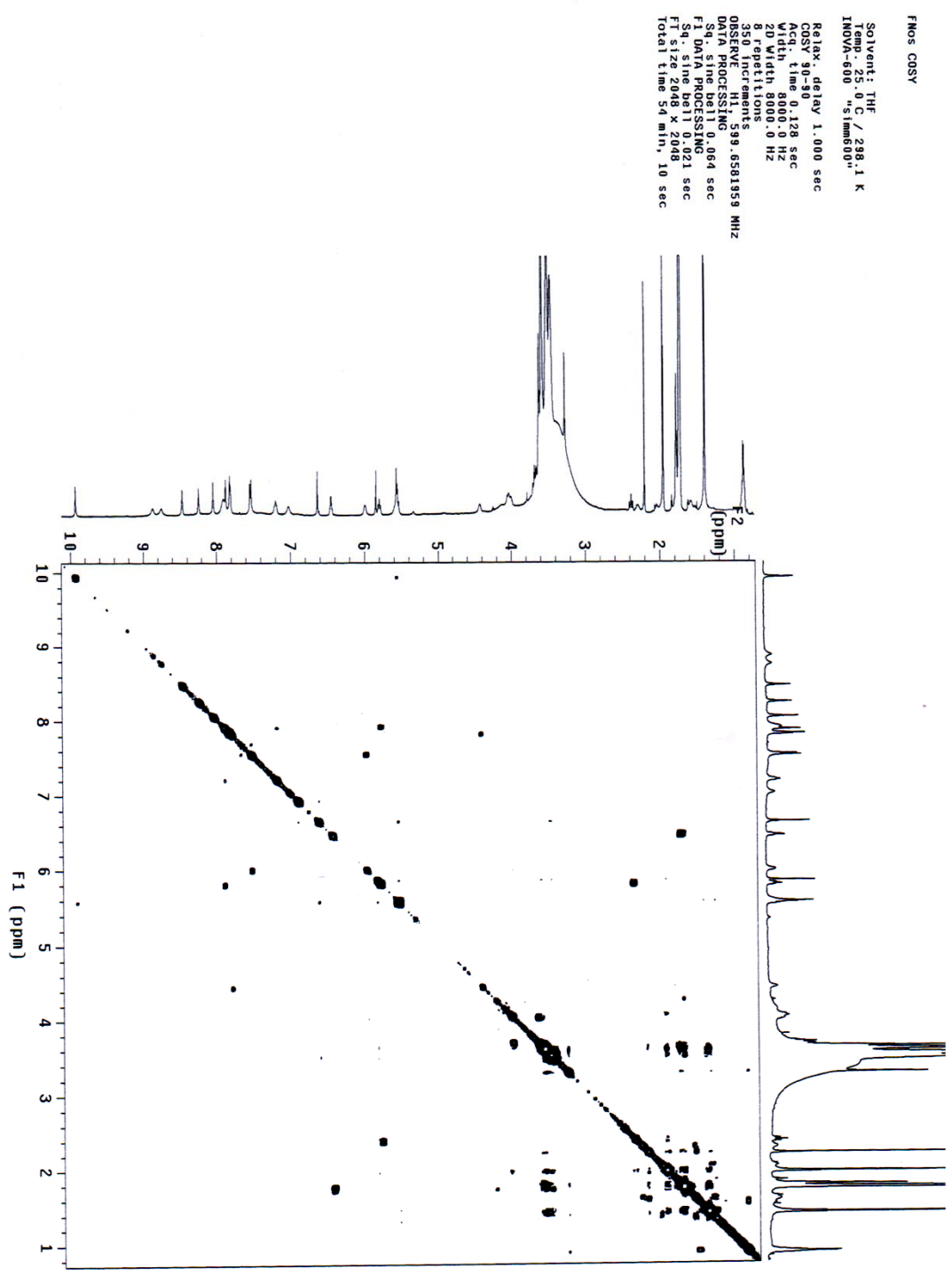
b



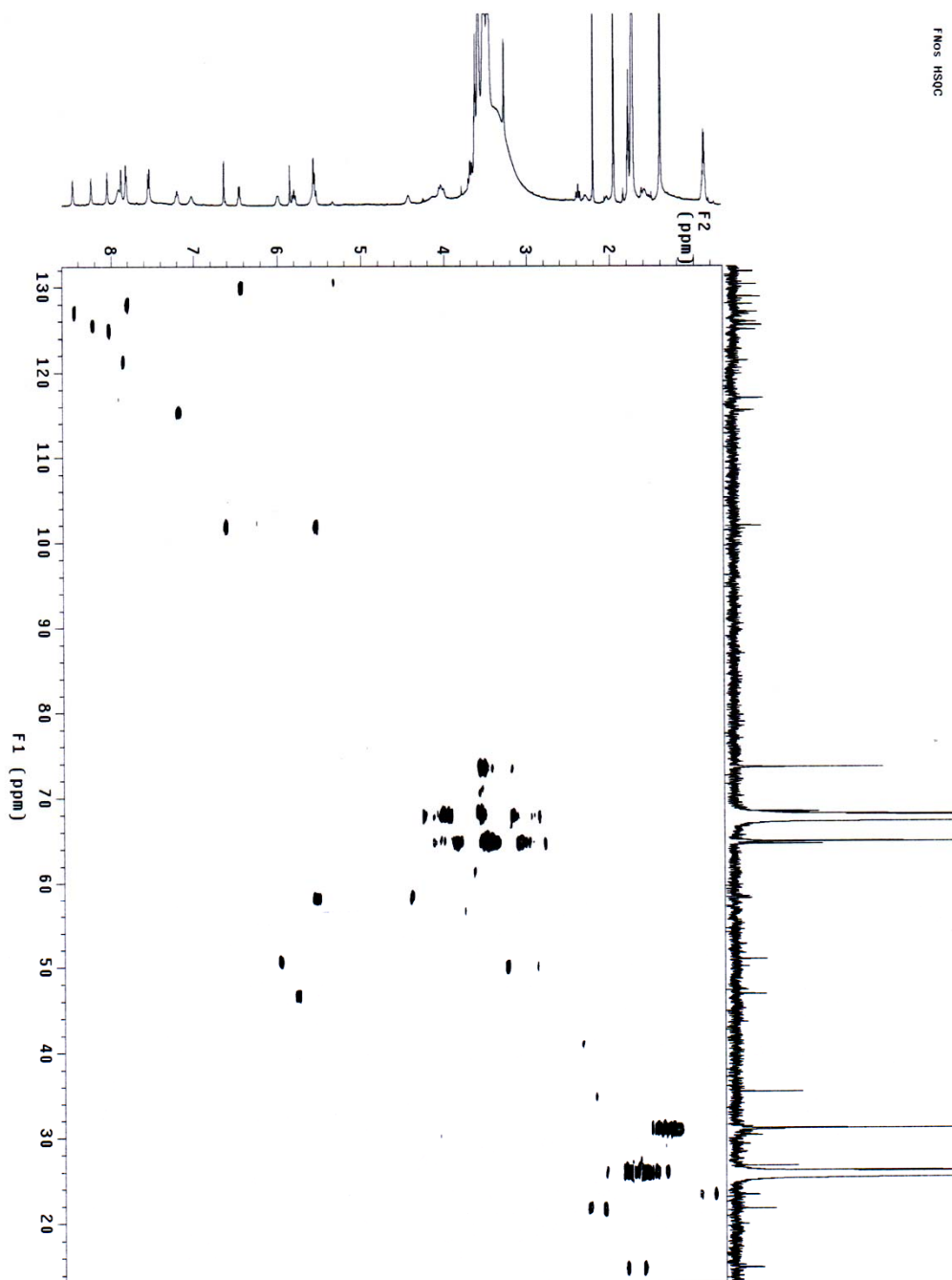
c



d



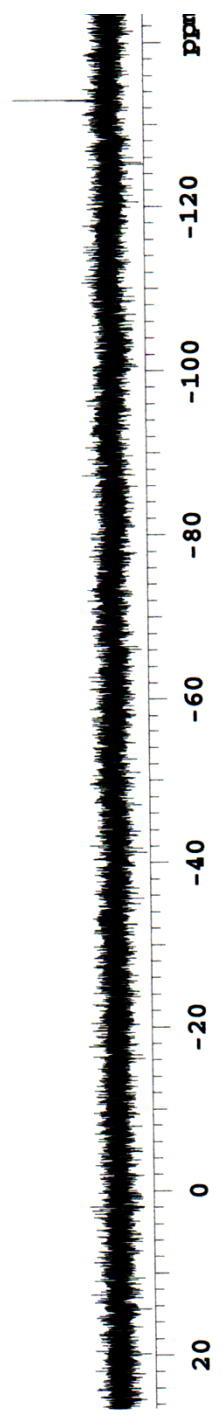
FNOS HSQC



e

f

-126.454



2.2 Supplementary Tables

Supplementary Table 1. Bacteria strains and plasmids used in this study

Stain/Plasmid	characteristics	Reference
Stains		
<i>Escherichia coli</i> DH5 α	Host for general cloning	Invitrogen
<i>E. coli</i> BL21 (ED3)	Host for protein expression	Invitrogen
<i>E. coli</i> ATCC 37845	<i>E. coli</i> containing a high copy number plasmid for producing tryptophan synthase from <i>Salmonella enterica</i>	ATCC, (8)
SL4100	BL21 (ED3) derivative, containing the vector pET28a	This study
SL4101	BL21 (ED3) derivative, containing pSL4101 for producing NosL	This study
SL4103	BL21 (ED3) derivative, containing pSL4103 for producing the C95A mutant NosL	This study
SL4105	BL21 (ED3) derivative, containing pSL4105 for producing the C99A mutant NosL	This study
SL4107	BL21 (ED3) derivative, containing pSL4107 for producing the C103A mutant NosL	This study
SL4109	BL21 (ED3) derivative, containing pSL4109 for producing the G142A mutant NosL	This study

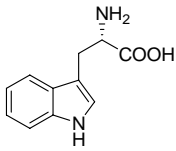
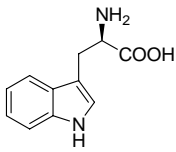
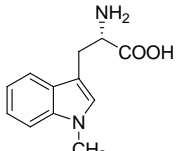
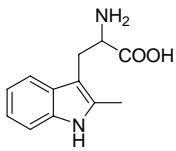
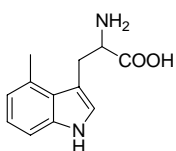
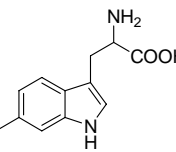
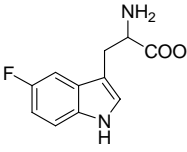
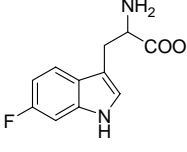
<i>Streptomyces actuosus</i>	NOS-producing strain	ATCC
ATCC 25421		
Plasmids		
pSP72	<i>E. coli</i> subcloning vector	Promega
pET28a	Vector for expression of 6x His-tagged protein in <i>E. coli</i>	Novagen
pSL4001	pOJ446-based cosmid that contains the NOS biosynthetic gene cluster.	(2)
pSL4100	pSP72 derivative, containing a 1.2 kb PCR product that encodes NosL	This study
pSL4101	pET28a derivative, containing a 1.2 kb PCR product that encodes NosL	This study
pSL4102	pSP72 derivative, containing a 1.2 kb PCR product that encodes the C95A mutant NosL	This study
pSL4103	pET28a derivative, containing a 1.2 kb PCR product that encodes the C95A mutant NosL	This study
pSL4104	pSP72 derivative, containing a 1.2 kb PCR product that encodes the C99A mutant NosL	This study
pSL4105	pET28a derivative, containing a 1.2 kb PCR product that encodes the C99A mutant NosL	This study
pSL4106	pSP72 derivative, containing a 1.2 kb PCR product that encodes the C102A mutant NosL	This study

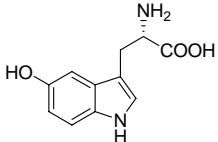
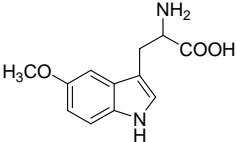
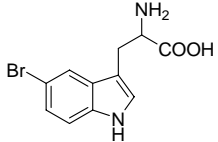
pSL4107	pET28a derivative, containing a 1.2 kb PCR product that encodes the C102A mutant NosL	This study
pSL4108	pSP72 derivative, containing a 1.2 kb PCR product that encodes the G142A mutant NosL	This study
pSL4109	pET28a derivative, containing a 1.2 kb PCR product that encodes the G142A mutant NosL	This study
pSL4110	pET28a derivative, containing a 531bp PCR product that encodes FldA	This study
pSL4111	pET28a derivative, containing a 747 bp PCR product that encodes Fpr	This study

Supplementary Table 2. Primers (shown from 5' to 3') used in this study. Restriction sites are underlined.

NosL-for	TTGAATTCATGACGCAGAACTCCCAGG (EcoRI)
NosL-rev	TTTAAGCTTTCAGACCGCCCGGGACGCCTC (HindIII)
NLC95A-for	CTACACCACCAACTACGCCGACTCCGAGTGCAAG
NLC95A-rev	CTTGCACTCGGAGTCGGCGTAGTTGGTGGTGTAG
NLC99A-for	CTACTGCGACTCCGAGGCCAAGATGTGCTCCATG
NLC995A-rev	CATGGAGCACATCTTGGCCTCGGAGTCGCAGTAG
NLC103A-for	CTCCGAGTGCAAGATGGCCTCCATGCGGAAGGGC
NLC103A-rev	GCCCTCCGCATGGAGGCCATCTTGCACTCGGAG
NLG142A-for	GGTCGGCTTCCTCACCGCCGAGTACGAGGACAAG
NLG142A-rev	CTTGTCTCGTACTCGGCGGTGAGGAAGCCGACC
NLE143D-for	GCTTCCTCACCGGCGACTACGAGGACAAGCACAC
NLE143D-rev	GTGTGCTTGTCTCGTAGTCGCCGGTGAGGAAGC
FldA-for	AAGAATTCATGGCTATCACTGGCATCTTTTTC (EcoRI)
FldA-rev	AAGTCGACTCAGGCATTGAGAATTCGTCG (Sall)
Fpr-for	TTTGAATTCATGGCTGATTGGGTAACAGGC (EcoRI)
Fpr-rev	TTTAAGCTTTTACCAGTAATGCTCCGCTGTC (HindIII)

Supplementary Table 3 Evaluation of the substrate specificity of NosL in the *nosL*-expressing *E. coli* strain SL4101.

Substrate(s)	Product(s)	Characteristic(s)
	MIA	Speeding up MIA production in the initial 4 hr, improved (~200%) in production compared to that of the control without the supplementation
	MIA	No effect on MIA production
	MIA	No effect on MIA production
	MIA	No effect on MIA production
	MIA	No effect on MIA production
	MIA	No effect on MIA production
	MIA and 5-fluoro-MIA	No effect on MIA production
	MIA and 6-fluoro-MIA	No effect on MIA production

	MIA	No effect on MIA production
	MIA	No effect on MIA production
	MIA	No effect on MIA production

Supplementary Table 4 Assignment of ^1H NMR and ^1H - ^{13}C correlations (HSQC) of 5'-fluoro-NOS (27).

Assignment	^{13}C	^1H chemical shift	Assignment	^{13}C	^1H chemical shift
But3	130.45	6.33 (q, J = 7.00)	Cys2	50.88	5.86 (m)
Py4	129.01	7.70 (s)	Glu2	46.80	5.69 (t, J = 10.50)
Thz (1) 5	128.10	7.72 (s)	Glu3	35.26	2.20 (m), 2.10 (m)
Thz (5) 5	127.20	8.32 (s)	Cys3	29.94	3.89 (m)
Thz (3) 5	125.66	8.13 (s)	Thr CH3	23.16	0.75 (d, J = 6.50)
Thz (2)5	125.13	7.93 (s)	Ind CH3	21.53	2.09 (s)
Thz(4)	121.52	7.77 (s)	But CH3	14.70	1.67 (d, J = 6.00)
Ind7	117.18	7.79 (m)	Ind NH		10.67 (s, br)
Ind6	115.64	7.09 (m)	Pyr OH		10.19 (s, br)
Deala3	102.00	6.52 E (s)	Deala NH		9.813 (s)
		5.45 Z (s)	But NH		8.76 (s)
Thr 3	68.01	3.0-3.8, overlapped with THF	Glu OH		8.63 (s,br)
Glu 4	64.57	3.0-3.8, overlapped with THF	Cys NH		7.43 (d, J = 9.50)
Thr 2	58.42	4.32 (m)	Thr NH		7.43 (d, J = 9.50)
Ind 4'	58.30	5.42 (m)	Thr OH		6.89 (br)

Supplementary Table 5 Minimum inhibitory concentrations (MICs) of NOS and 5'-fluoro-NOS (27).

Organism	Number^a	MIC (µg/ml)	
		NOS	5'-fluoro-NOS
<i>Bacillus subtilis</i>	SIPI-JD1001	0.008	0.004

^a The test organisms were deposited at Shanghai Institute of Pharmaceutical Industry (SIPI) with the given numbers.

3. Supplementary References

1. Sambrook, J. & Russell, D.W. *Molecular Cloning: A Laboratory Manual*, 3rd ed (Cold Spring Harbor Laboratory Press, New York, 2001).
2. Yu, Y. *et al.* Nosiheptide biosynthesis featuring a unique indole side ring formation on the characteristic thiopeptide framework. *ACS Chem. Biol.* **4**, 855-864 (2009).
3. Kennedy, M.C. *et al.* Evidence for the formation of a linear [3Fe-4S] cluster in partially unfolded aconitase. *J. Biol. Chem.* **259**, 14463-14471 (1984).
4. Beinert, H. Semi-micro methods for analysis of labile sulfide and of labile sulfide plus sulfane sulfur in unusually stable iron sulfur proteins. *Anal. Biochem.* **131**, 373-378 (1983).
5. Houck, D.R., Chen, L.C., Keller, P.J., Beale, J.M. & Floss, H.G. Biosynthesis of the modified peptide antibiotic nosiheptide in *Streptomyces-actuosus*. *J. Am. Chem. Soc.* **110**, 5800-5806 (1988).
6. Goss, R.J.M. & Newill, P.L.A. A convenient enzymatic synthesis of L-halotryptophans. *Chem. Commun.* **47**, 4924-4925 (2006).
7. Rydon, H.N. The synthesis of the nuclear-C-methylated tryptophans - a note on the aldehyde reactions for tryptophan. *J. Chem. Soc.* **2**, 705-710 (1948).
8. Hohenberg, P. & Kohn, W. Inhomogeneous electron gas. *Phys. Rev.* **136**, B864-B871 (1964).
9. Kohn, W. & Sham, L.J. Self-consistent equations including exchange and correlation effects. *Phys. Rev.* **140**, A1133 (1965).
10. Frisch, M.J. *et al.* *Gaussian 03, Revision C.02* (Gaussian Inc., Wallingford CT, 2004).
11. Becke, A.D. Density-functional thermochemistry .3. The role of exact exchange. *Chem.Phys.* **98**, 5648-5652 (1993).

12. Lee, C.T., Yang, W.T. & Parr, R.G. Development of the colle-salvetti correlation-energy formula into a functional of the electron-density. *Phys. Rev.* **B37**, 785-789 (1988).
13. Cancès, E. Mennucci, B. & Tomasi, J. A new integral equation formalism for the polarizable continuum model: theoretical background and applications to isotropic and anisotropic dielectrics. *J. Chem. Phys.* **107**, 3032-3041 (1997).
14. Cossi, M., Barone, V., Mennucci, B. & Tomasi, J. Ab initio study of ionic solutions by a polarizable continuum dielectric model. *Chem. Phys. Lett.* **286**, 253-263 (1998).
15. Pucci, M.J. *et al.* Antimicrobial evaluation of nocathiacins, a thiazole peptide class of antibiotics. *Antimicrob. Agents. Chemother.* **48**, 3697-3701 (2004).
16. McFarland, J. The nephelometer - an instrument for estimating the number of bacteria in suspensions used for calculating the opsonic index and for vaccines. *J. Am. Med. Assoc.* **49**, 1176-1178 (1907).